

Isolation and sequence-based characterization of a koala symbiont: *Lonepinella koalarum*

Katherine E Dahlhausen¹, Guillaume Jospin¹, David A Coil¹, Jonathan A Eisen^{1,2,3}, Laetitia G E Wilkins^{Corresp. 1}

¹ Genome and Biomedical Sciences Facility, University of California, Davis, Davis, California, United States

² Department of Evolution and Ecology, University of California, Davis, Davis, California, United States

³ Department of Medical Microbiology and Immunology, University of California, Davis, Davis, California, United States

Corresponding Author: Laetitia G E Wilkins
Email address: megaptera.helvetiae@gmail.com

Koalas (*Phascolarctos cinereus*) are highly specialized herbivorous marsupials that feed almost exclusively on *Eucalyptus* leaves, which are known to contain varying concentrations of many different toxic chemical compounds. The literature suggests that *Lonepinella koalarum*, a bacterium in the Pasteurellaceae family, can break down some of these toxic chemical compounds. Furthermore, in a previous study, we identified *L. koalarum* as the most predictive taxon of koala survival during antibiotic treatment. Therefore, we believe that this bacterium may be important for koala health. Here, we isolated a strain of *L. koalarum* from a healthy koala female and sequenced its genome using a combination of short-read and long-read sequencing. We placed the genome assembly into a phylogenetic tree based on 120 genome markers using the Genome Taxonomy Database (GTDB), which currently does not include any *L. koalarum* assemblies. Our genome assembly fell in the middle of a group of *Haemophilus*, *Pasteurella* and *Basfia* species. According to average nucleotide identity and a 16S rRNA gene tree, the closest relative of our isolate is *L. koalarum* strain Y17189. Then, we annotated the gene sequences and compared them to 55 closely related, publicly available genomes. Several genes that are known to be involved in carbohydrate metabolism could exclusively be found in *L. koalarum* relative to the other taxa in the pangenome, including glycoside hydrolase families GH2, GH31, GH32, GH43 and GH77. Among the predicted genes of *L. koalarum* were 79 candidates putatively involved in the degradation of plant secondary metabolites. Additionally, several genes coding for amino acid variants were found that had been shown to confer antibiotic resistance in other bacterial species against pulvomycin, beta-lactam antibiotics and the antibiotic efflux pump KpnH. In summary, this genetic characterization allows us to build hypotheses to explore the potentially beneficial role that *L. koalarum* might play in the koala intestinal microbiome. Characterizing and understanding beneficial symbionts at the whole genome level is important for the

development of anti- and probiotic treatments for koalas, a highly threatened species due to habitat loss, wildfires, and high prevalence of *Chlamydia* infections.

1 **Isolation and sequence-based characterization of a koala symbiont:**

2 ***Lonepinella koalarum***

3

4 Katherine E. Dahlhausen¹, Guillaume Jospin¹, David A. Coil¹, Jonathan A. Eisen^{1,2,3}, and
5 Laetitia G. E. Wilkins¹

6

7 ¹ Genome and Biomedical Sciences Facility, University of California, Davis, Davis, CA 95616,
8 USA

9 ² Department of Evolution and Ecology, University of California, Davis, Davis, CA 95616, USA

10 ³ Department of Medical Microbiology and Immunology, University of California, Davis, Davis,
11 CA 95616, USA

12

13 Corresponding Author:

14 Laetitia Wilkins¹

15 451 Health Science Drive

16 Genome and Biomedical Sciences Facility

17 University of California, Davis

18 Davis, CA, 95616, United States

19 Email address: megaptera.helvetiae@gmail.com

20 Abstract

21 Koalas (*Phascolarctos cinereus*) are highly specialized herbivorous marsupials that feed almost
22 exclusively on *Eucalyptus* leaves, which are known to contain varying concentrations of many
23 different toxic chemical compounds. The literature suggests that *Lonepinella koalarum*, a
24 bacterium in the Pasteurellaceae family, can break down some of these toxic chemical
25 compounds. Furthermore, in a previous study, we identified *L. koalarum* as the most predictive
26 taxon of koala survival during antibiotic treatment. Therefore, we believe that this bacterium
27 may be important for koala health. Here, we isolated a strain of *L. koalarum* from a healthy koala
28 female and sequenced its genome using a combination of short-read and long-read sequencing.
29 We placed the genome assembly into a phylogenetic tree based on 120 genome markers using
30 the Genome Taxonomy Database (GTDB), which currently does not include any *L. koalarum*
31 assemblies. Our genome assembly fell in the middle of a group of *Haemophilus*, *Pasteurella* and
32 *Basfia* species. According to average nucleotide identity and a 16S rRNA gene tree, the closest
33 relative of our isolate is *L. koalarum* strain Y17189. Then, we annotated the gene sequences and
34 compared them to 55 closely related, publicly available genomes. Several genes that are known
35 to be involved in carbohydrate metabolism could exclusively be found in *L. koalarum* relative to
36 the other taxa in the pangenome, including glycoside hydrolase families GH2, GH31, GH32,
37 GH43 and GH77. Among the predicted genes of *L. koalarum* were 79 candidates putatively
38 involved in the degradation of plant secondary metabolites. Additionally, several genes coding
39 for amino acid variants were found that had been shown to confer antibiotic resistance in other
40 bacterial species against pulvomycin, beta-lactam antibiotics and the antibiotic efflux pump
41 KpnH. In summary, this genetic characterization allows us to build hypotheses to explore the
42 potentially beneficial role that *L. koalarum* might play in the koala intestinal microbiome.
43 Characterizing and understanding beneficial symbionts at the whole genome level is important
44 for the development of anti- and probiotic treatments for koalas, a highly threatened species due
45 to habitat loss, wildfires, and high prevalence of *Chlamydia* infections.

46

47 Introduction

48 Koalas (*Phascolarctos cinereus*) are arboreal marsupials that are highly specialized herbivores in
49 that they feed almost exclusively on the foliage of select *Eucalyptus* species (Moore & Foley,
50 2005; Callaghan et al., 2011). All *Eucalyptus* species contain chemical defenses against

51 herbivory that include tannins, B-ring flavanones, phenolic compounds, terpenes, formylated
52 phloroglucinols, cyanogenic glucosides, and other plant secondary metabolites (Lawler, Foley &
53 Eschler, 2000; Gleadow et al., 2008; Brice et al., 2019; Liu et al., 2019). Plant chemical defenses
54 can deter herbivores by affecting taste and/or digestibility of ingested material, with varying
55 levels of toxic effects (Brice et al., 2019). These defenses and anti-nutrient compounds, which
56 will be referred to generally as ‘PCDs’ (for plant chemical defenses) hereafter, are very common,
57 and there is well-established evidence that herbivores can overcome these defenses in their diet
58 at least in part via PCD-degradation by their intestinal microbial communities (Freeland &
59 Janzen, 1974; Waterman et al., 1980; Hammer & Bowers, 2015; Kohl & Denise Dearing, 2016).
60 However, it is unknown to what extent *Eucalyptus* PCDs are degraded by the intestinal microbial
61 communities of koalas.

62

63 Research has highlighted several ways in which koalas are able to manage such a toxic diet
64 independent of the functions of their intestinal microbial communities. For example, some
65 studies suggest that koalas can minimize PCDs intake through tree- and even leaf selection
66 (Lawler, Foley & Eschler, 2000; Marsh et al., 2003; Moore & Foley, 2005; Liu et al., 2019).
67 Another study identified several genes in the koala genome that are associated with metabolism
68 and detoxification of many types of xenobiotics (Johnson et al., 2018). The findings from a study
69 on microsomal samples from koala liver also suggest that koalas are able to metabolize some
70 xenobiotics in their livers (Ngo et al., 2000). Furthermore, other research suggests that toxic
71 compounds found in *Eucalyptus* may be absorbed in the upper digestive system before they even
72 reach the intestinal microbial community of herbivores (Foley, Lassak & Brophy, 1987).

73

74 The intestinal microbial communities of koalas are also thought to contribute to the management
75 and degradation of PCDs found in *Eucalyptus* leaves. To date, the most compelling evidence for
76 this is included in a recent study on the koala fecal microbiome, which identified several
77 metabolic pathways and relevant bacterial species proposed to be important in detoxification
78 processes (Shiffman et al., 2017). The koala microbiome as a whole has shown to play an
79 important role in macro nutrient digestion and fiber degradation (Blyton et al., 2019; Brice et al.,
80 2019). Moreover, there is evidence that the koala gastrointestinal microbiome can influence diet
81 selection of individual hosts (Blyton et al., 2019). At the individual level, several bacterial

82 isolates associated with the intestinal microbial communities of koalas have been characterized
83 in the context of degradation of PCDs found in *Eucalyptus* leaves (Osawa, 1990, 1992; Osawa et
84 al., 1993, 1995; Looft, Levine & Stanton, 2013). One of these cultured isolates is a bacterium
85 known as *Lonepinella koalarum*. It had been first isolated from the mucus around the caecum in
86 koalas and was shown to degrade tannin-protein complexes that can be found in *Eucalyptus*
87 leaves (Osawa et al., 1995; Goel et al., 2005). Briefly, tannin-protein complexes are extremely
88 diverse and result from the reaction between plant defense secondary metabolites; *i.e.*, tannins,
89 and proteins. Tannins bind proteins followed by the formation of a precipitate, which cannot be
90 digested by koalas or utilized by microbes (Adamczyk et al., 2017). In our previous work, *L.*
91 *koalarum* was identified as the most predictive taxon of koala survival during antibiotic
92 treatment (Dahlhausen et al., 2018). Briefly, a co-occurrence network analysis identified four
93 bacterial taxa, including one of the genus *Lonepinella*, that could be found in feces of koalas that
94 survived their antibiotic treatment after *Chlamydia* infection. However, these four taxa were
95 absent from feces of koalas that died. Furthermore, in the same study a random forest analysis
96 revealed that the most predictive taxon of whether a koala would live or die during their
97 antibiotic treatment was identified as *L. koalarum*. This finding suggests that *L. koalarum* could
98 be important for koala health, but the study did not present any evidence relating to PCD
99 degradation in the highly specialized diet of koalas.

100

101 It is well understood that animals with highly specialized diets also are likely to have highly
102 specialized intestinal microbial communities (Higgins et al., 2011; Kohl et al., 2014; Alfano et
103 al., 2015; Kohl, Stengel & Denise Dearing, 2016). Disturbances of a specialized microbial
104 community, such as the introduction of antibiotics, can have profound effects on the host's health
105 (Kohl & Denise Dearing, 2016; Brice et al., 2019). Yet, koalas are regularly treated with
106 antibiotics due to the high prevalence of *Chlamydia* infections in many populations
107 (Polkinghorne, Hanger & Timms, 2013). While recent advances in *Chlamydia pecorum* vaccines
108 for koalas are a promising alternative for managing koala populations, antibiotics are still the
109 current treatment method for bacterial infections in koalas (Waugh et al., 2016; Desclozeaux et
110 al., 2017; Nyari et al., 2018). The antibiotics used in practice might not only target *Chlamydia*
111 *pecorum* but also beneficial koala gut symbionts as a side effect. Therefore, it is important to
112 learn about bacteria associated with koala health, such as *L. koalarum*, in order to further the

113 development of alternative treatments for bacterial infections in koalas and to recommend
114 antibiotic compounds that are potentially less disruptive to members of the koala gut
115 microbiome.

116

117 Here we isolated a strain of *L. koalarum* (hereafter called strain UCD-LQP1) from the feces of a
118 healthy koala (*P. cinereus*) female at the San Francisco Zoo. We sequenced the genome of *L.*
119 *koalarum* UCD-LQP1 using a combination of long- and short-read sequencing, and then
120 assembled and annotated the genome. We compared the genome assembly to the most closely
121 related genomes that are currently publicly available. The genome assembly of *L. koalarum*
122 UCD-LQP1 was placed in a phylogenetic tree and screened for genes putatively involved in the
123 degradation of plant secondary metabolites, carbohydrate metabolism, and antibiotic resistance.
124 Additionally, we identified and characterized putative genes that were unique to this strain and
125 two recently sequenced genomes of *L. koalarum* from Australia.

126

127 **Materials and methods**

128 *Sampling of koala feces and preparation of culturing media*

129 A koala fecal pellet was collected, with permission from the San Francisco Zoo, from a healthy,
130 adult, captive, female koala (*Phascolarctos cinereus*). We do not have any information on the
131 geographical origin of this koala. Koalas at the SF Zoo are fed blue gum leaves (*Eucalyptus*
132 *globulus*), which grow quite abundantly in California. Jim Nappi and Graham Crawford of the
133 San Francisco Zoo organized and permitted koala fecal sample collection. The fresh fecal pellet
134 was collected from the floor with sterilized tweezers and stored in a sterile 15 ml Falcon tube
135 (Thermo Fisher Scientific, USA). The tube was immediately placed on ice after collection and
136 subsequently stored at 4° C overnight.

137

138 The preparation of the *Lonepinella koalarum* culturing media was modified from methods
139 developed by Osawa et al. (1995). A 2 % agarose (Fisher BioReagents, USA) solution of
140 Bacto™ Brain Heart Infusion (BHI; BD Biosciences, USA) was prepared following
141 manufacturer protocols. After the media had solidified in petri dishes, a 2 % tannic acid solution
142 was prepared by combining 1 g of tannic acid powder per 50 ml of sterile Nanopure™ water
143 (Spectrum Chemical MFG CORP, USA). The solution was vortexed for 1 min until

144 homogenized, resulting in a brown, transparent liquid. Using a sterile serological pipette, 5 ml of
145 the 2 % tannic acid solution was gently added to each BHI media plate and left for 20 min. After
146 incubation, the remaining liquid on the plate was decanted. No antibiotic compounds were added
147 to the medium.

148 *Culturing of isolates and DNA extraction*

149 The koala fecal pellet was cut in half with sterile tweezers. Tweezers were re-sterilized and used
150 to move approximately 300 mg of material from the center of the pellet to a sterile 2 ml
151 Eppendorf tube containing 1 ml of sterile, Nanopure™ water. The tube was vortexed for 3 min,
152 intermittently checking until the solution was homogenized into a slurry. One hundred µl of the
153 homogenized fecal slurry was micro-pipetted onto to a BHI+tannin plate and stored in an
154 anaerobic chamber (BD GasPak™ EZ anaerobe chamber system; BD Biosciences, USA) at 37°
155 C for 3 days. Each individual colony that grew was plated onto a freshly made BHI+tannin plate
156 using standard dilution streaking techniques. The new plates were stored in an anaerobic
157 chamber at 37 °C for another 3 days. This step was repeated two more times to decrease the
158 probability of contamination or co-culture.

159

160 An individual colony from each of the plates from the third round of dilution streaking was
161 moved to a sterile 30 ml glass culture tube containing 5 ml of sterile Bacto™ BHI liquid media
162 (prepared following manufacturer protocol; BD Biosciences, USA). Each tube was then capped
163 with a sterile rubber stopper and purged with nitrogen gas in order to create an anaerobic
164 environment. The tubes were placed in an incubated orbital shaker (ThermoFisher Scientific
165 MaxQ™ 4450) for 3 days at 37 °C at 250 rpm.

166

167 Using a sterile serological pipette, 1.8 ml of each liquid culture was transferred to a sterile 2 ml
168 Eppendorf tube. The tubes were spun at 13,000 g for 2 min and the supernatant was carefully
169 decanted. The DNA was extracted from the pellet in each sample with the Promega Wizard
170 Genomic DNA Purification Kit (Promega, USA) according to the manufacturer's protocol. DNA
171 was eluted in a final volume of 100 µl and stored at 4 °C.

172 *PCR and Sanger sequencing*

173 PCR amplification of the 16S rRNA gene was performed on each of the eluted DNA samples.
174 PCR reactions were prepared using the bacteria-specific “universal” primer pair 27F (5’-
175 AGAGTTTGATCMTGGCTCAG-3’; Stackebrandt & Goodfellow, 1991) and 1391R (5’-
176 GACGGGCGGTGTGTRCA-3’; Turner et al., 1999). PCR amplifications were performed in a
177 BioRad T100™ Thermal Cycler in 50 µl reactions. Each reaction contained 2 µl of the eluted
178 DNA from the aforementioned extraction, 5 µl of 10x Taq buffer (Qiagen, USA), 10 µl of Q
179 buffer (Qiagen), 1.25 µl of 10mM dNTPs (Qiagen), 2.5 µl of 10mM 27F primer, 2.5 µl of 10mM
180 1391R primer, 0.3 µl of Taq polymerase (Qiagen), and 26.45 µl of sterile water. The cycling
181 conditions were: (1) 95 °C for 3 min, (2) 40 cycles of 15 sec at 95 °C, 30 sec at 54 °C, and 1 min
182 at 72 °C, (3) a final incubation at 72 °C for 5 min, and (4) holding at 12 °C upon completion.

183

184 The PCR product for each sample was purified and concentrated by following the
185 manufacturer’s protocol for the NucleoSpin Gel and PCR Clean-up kit (Macherey-Nagel, USA).
186 The purified PCR product for each sample was quantified by following the manufacturer’s
187 protocol for the Qubit dsDNA HS Assay Kit (Thermo Fisher Scientific, USA). The PCR product
188 for each sample was then diluted to 26 ng/µl and submitted for forward and reverse Sanger
189 sequencing at the University of California Davis DNA Sequencing Facility. The program
190 SeqTrace version 0.9.0 (Stucky, 2012) was used to edit and create consensus sequences of the
191 reads received from the sequencing facility, following the protocol detailed in Dunitz et al.
192 (2015). The consensus sequence for each sample was uploaded to the NCBI blast website for
193 organism identification (Madden, 2003). The DNA of one of the isolates that had been identified
194 as *L. koalarum* was used for whole-genome sequencing, as described below. We refer to this
195 isolate as *L. koalarum* strain UCD-LQP1.

196 *Whole genome sequencing and assembly*

197 DNA from one sample identified as *L. koalarum* strain UCD-LQP1 was submitted for whole
198 genome PacBio sequencing at SNPsaurus. After sequencing, the demultiplexed bam file was
199 tested for reads that contained palindromic sequences since a preliminary assembly with Canu
200 version 1.8 (Koren et al., 2017) indicated the presence of adapter sequences. Palindromic reads
201 were split in half, aligned with minimap2 (an executable in Canu), and those palindromic reads

202 that aligned over at least two-thirds of the split read were reduced to the first part of the
203 palindrome (Koren et al., 2017). This procedure efficiently removed adapter sequences. These
204 adapter-free reads were used in the hybrid assembly described below.

205

206 The same DNA that had been used for PacBio sequencing was also submitted for Illumina
207 sequencing. Ten ng of genomic DNA were used in a 1:10 reaction of the Nextera DNA Flex
208 Library preparation protocol (Illumina, USA). Fragmented DNA was amplified with Phusion
209 DNA polymerase (New England Biolabs) in 12 PCR cycles with 1 min extension time. Samples
210 were sequenced on a HiSeq4000 instrument (University of Oregon GC3F) with paired-end 150
211 bp reads. The 10,309,488 raw reads were quality controlled and filtered for adaptors and PhiX
212 using the Joint Genome Institute's BBDuk tool version 37.68 (Bushnell, 2014), resulting in
213 10,302,312 reads. The 308 cleaned PacBio reads and 10,302,312 filtered Illumina reads were
214 combined with all default parameters of Unicycler version 0.4.5, a tool used to assemble
215 bacterial genomes from both long and short reads (Wick et al., 2017).

216 *Genome annotation*

217 Completeness and contamination of the *L. koalarum* strain UCD-LQP1 assembly were
218 determined with CheckM version 1.0.8 (Parks et al., 2015), number of contigs, total length,
219 GC%, N50, N75, L50, and L75 were determined with QUAST (Quality Assessment Tool for
220 Genome Assemblies; Gurevich et al., 2013), and the assembly was annotated with PROKKA
221 version 1.12 (Seemann, 2014). The *L. koalarum* strain UCD-LQP1 genome assembly was
222 uploaded to the Rapid Annotation using Subsystem Technology online tool (RAST), a genome
223 annotation program for bacterial and archaeal genomes (Aziz et al., 2008). The SEED viewer in
224 RAST was used to browse features of the genome (Overbeek et al., 2014). To screen the *L.*
225 *koalarum* strain UCD-LQP1 assembly for genes putatively involved in tannin degradation and
226 xenobiotic metabolisms; *i.e.*, the degradation of plant secondary metabolites, coding regions in
227 the assembly were identified using Prodigal version 2.6.3 (Hyatt et al., 2010). Each identified
228 coding region was annotated using eggNOG (a database of orthologous groups and functional
229 annotation that is updated more regularly than PROKKA) mapper version 4.5.1 (Jensen et al.,
230 2008). Then, KEGG (Kyoto Encyclopedia of Genes and Genomes) pathways putatively involved
231 in xenobiotics biodegradation and metabolism, were extracted from the eggNOG annotations

232 (Class 1.11 Xenobiotics biodegradation and metabolism includes the following KEGG pathways:
233 ko00362, ko00627, ko00364, ko00625, ko00361, ko00623, ko00622, ko00633, ko00642,
234 ko00643, ko00791, ko00930, ko00363, ko00621, ko00626, ko00624, ko00365, ko00984,
235 ko00980, ko00982, and ko00983 (Kanehisa & Goto, 2000)), and the corresponding nucleotide
236 sequences from the *L. koalarum* genome assemblies were saved. Individual genes with hits in
237 KEGG pathways were manually mapped onto KEGG reference maps using the KEGG webtool
238 (Kanehisa & Goto, 2000).

239 *16S rRNA gene based phylogenetic placement of genome*

240 The 16S rRNA gene sequence within the genome assembly was extracted from RAST by
241 searching for ‘ssu rRNA’ in the function search of the SEED genome browser (Aziz et al., 2008;
242 Overbeek et al., 2014). Following the protocol outlined in Dunitz et al. (2015), the 16S rRNA
243 gene sequence was uploaded to the Ribosomal Database Project (RDP; Cole et al., 2014) and
244 grouped with all 16S rRNA gene sequences in the Pasteurellaceae family and one chosen
245 outgroup, *Agarivoran* spp., to root the tree. The taxon names from the RDP output file were
246 manually cleaned up and their 16S rRNA gene sequences were used to build a phylogenetic tree
247 with the program FastTree (Price, Dehal & Arkin, 2009). Nodes and tip labels were manually
248 edited for Figure 1 in iTOL (interactive tree of life; web tool; Letunic & Bork, 2019). The 16S
249 rRNA gene sequence alignment (Wilkins & Coil, 2020a) and its resulting phylogenetic tree are
250 available on Figshare (Wilkins & Coil, 2020b). During the preparation of this manuscript, two
251 more *L. koalarum* type strains had their genomes sequenced: one by the DOE Joint Genome
252 Institute, USA (GenBank accession number GCA_004339625.1; 2,486,773 bp long) and one by
253 the Maclean Lab in Australia (GenBank accession number GCA_004565475.1; 2,509,358 bp).
254 Both assemblies were based on type strains originating from the same isolation of *L. koalarum* in
255 1995 (Osawa et al., 1995), DSM 10053 and ATCC 700131, respectively. These two *L. koalarum*
256 genome assemblies were henceforth included in our analysis. When we refer to all three *L.*
257 *koalarum* genome assemblies, we simply say ‘in *L. koalarum*’ and when we refer to the strain
258 sequenced in this study, we use ‘the assembly of *L. koalarum* strain UCD-LQP1’.

259 *Comparative genomics*

260 The GTDB-Tk software toolkit version 0.3.0 (Chaumeil, Hugenholtz & Parks, 2018) of the
261 Genome Taxonomy Database (GTDB) project was chosen to place *L. koalarum* into a pre-
262 generated conserved marker gene tree using 120 marker genes (Parks et al., 2018). After placing
263 the assembly into the GTDB tree, a clade in the tree was extracted that contained *L. koalarum*
264 strain UCD-LQP1 and 55 other taxa, of which all members belonged to the order Pasteurellales.
265 This clade contained all sequenced genomes of the closest neighboring taxa ($n = 55$) to *L.*
266 *koalarum* in the GTDB tree at the time of this analysis (3rd of August 2019). All of these 55
267 genomes were downloaded from GenBank (using the accession numbers in the GTDB) to
268 perform a comparative genomic analysis in Anvi'o version 5.5 (Eren et al., 2015). The two other
269 *L. koalarum* genomes from GenBank were included in the following analysis as well. Accession
270 numbers of all genome assemblies included can be found in Supplementary Table S1 ($n = 58$).
271 The Anvi'o workflow for microbial pangenomics was followed (Delmont & Eren, 2018). The
272 blastp program from NCBI was used for a gene search (Altschul et al., 1990), the Markov
273 Cluster algorithm (MCL) version 14.137 (van Dongen & Abreu-Goodger, 2012) was used for
274 clustering, and the program MUSCLE was used for alignment (Edgar, 2004). An inflation
275 parameter of 6 was chosen to identify clusters in amino acid sequences. Genomes in the
276 pangenome of Anvi'o were ordered based on a genomic marker gene tree. This tree was built in
277 PhyloSift version 1.0.1 (Darling et al., 2014) with its updated markers database (version 4,
278 posted on 12th of February 2018; Jospin, 2018) for the alignment. We used RAxML version
279 8.2.10 on the CIPRES web server for the tree inference (Miller, Pfeiffer & Schwartz, 2010)
280 following the analysis in (Wilkins et al., 2019). Gene clusters in Anvi'o were ordered based on
281 presence/absence. We also used Anvi'o to compute average nucleotide identities across the
282 genomes with PyANI (Pritchard et al., 2016). In the heatmap, ANI values $> 95\%$ (and $>70\%$ for
283 a separate figure, respectively) were colored in red.

284

285 Gene clusters from the Anvi'o microbial pangenomics analysis that could only be found in the
286 three *L. koalarum* genome assemblies were extracted. Then, we also extracted all gene clusters
287 that could only be found in the assembly of *L. koalarum* strain UCD-LQP1. Partial sequences
288 were removed. A literature search of the remaining genes was conducted to identify possible

289 roles *L. koalarum* might play in the gut microbiome of koalas. Tables were summarized in R
290 version 3.4.0 (R Development Core Team, 2013).

291 *Carbohydrate metabolism*

292 Since the majority of gene clusters unique to *L. koalarum* genome assemblies fell into the COG
293 (Clusters of Orthologous Groups) category ‘Carbohydrate metabolism’, we decided to screen all
294 three assemblies against the Carbohydrate-Active Enzymes Database (CAZy), an expert resource
295 for glycogenomics (Cantarel et al., 2009; Lombard et al., 2014). In brief, CAZy domains were
296 identified based on CAZy family HMMs (Hidden Markov Models) with a coverage of >95% and
297 an e-value < 1e-15. Searches were done through dbCAN, a web resource for automated
298 carbohydrate-active enzyme annotation (Yin et al., 2012) and CAZy hits were only retained if
299 they had been found with all three search tools. The three search tools included (i) HMMER
300 version 3.3 (Eddy, 1998), (ii) DIAMOND version 0.9.29 for fast blast hits in the CAZy database
301 (Buchfink, Xie & Huson, 2015; default parameters; *i.e.*, e-value < 1e-102, hits per query (-k) =
302 1), and (iii) Hotpep version 1 for short, conserved motifs in the PPR (Peptide Pattern
303 Recognition) library (Busk et al., 2017; default parameters; *i.e.*, frequency > 2.6, hits > 6). For a
304 detailed walk-through of the assembly, annotation, search for KEGG pathways, and comparative
305 genomics analyses, please refer to the associated Jupyter notebook (Wilkins, 2020a).

306 *Identification of antibiotic resistance genes*

307 All three *L. koalarum* genome assemblies were uploaded to the Comprehensive Antibiotic
308 Resistance Database (CARD version 3.0.7; Jia et al., 2017) and the ResFinder database version
309 5.1.0 (Zankari et al., 2012) to screen them for putative antibiotic resistance genes and their
310 variants using blastn searches against CARD 2020 reference sequences using default parameters.
311 The Resistance Gene Identifier (RGI) search pipeline was used to detect SNPs (single nucleotide
312 polymorphisms) using the ‘perfect, strict, complete genes only’ criterion on their website.
313 Briefly, antibiotic resistance genes were searched with nucleotide sequences as input. RGI first
314 predicts complete open reading frames (ORFs) using Prodigal version 2.6.3. To find protein
315 homologs in the CARD references, DIAMOND version 0.9.29 is used. The ‘perfect’ algorithm
316 detects perfect matches of individual amino acids to positions in the curated reference sequences

317 that had been previously associated with antibiotic resistance in other bacterial species (Alcock
318 et al., 2020).

319

320 **Results and discussion**

321 *Identification of isolates*

322 Besides the isolates identified as *L. koalarum*, we had several other colonies growing on the
323 BHI+tannin plates, including isolates with 16S rRNA gene sequences that matched *Bacillus*
324 *cereus*, *Bacillus nealsonii*, *Bacillus sonorensis*, and *Escherichia coli*. *E. coli* was the most
325 common species isolated.

326

327 *Assembly taxonomy and gene annotation*

328 The hybrid assembly generated was 2,608,483 bp in length with an N50 of 2,299,135 bp and a
329 coverage of 672. According to the marker gene analysis in CheckM, the assembly was 99.21%
330 complete and less than 1% contaminated with a GC content of 39.02% (see Table 1 for
331 additional details). One contig in the assembly appears to be a 3,899 bp long plasmid. This is
332 indicated by circularity of that contig and positive matches to plasmids in related taxa when
333 uploaded to the NCBI blast website for organism identification (Madden, 2003). The two most
334 similar sequences on GenBank were a 71 percent similar sequence of *Pasteurella multocida*
335 strain U-B411 plasmid pCCK411 (accession number FR798946.1) and a 70 percent similar
336 sequence of *Mannheimia haemolytica* strain 48 plasmid pKKM48 (accession number
337 MH316128.1). The putative plasmid sequence was deposited on FigShare (Wilkins & Jospin,
338 2020).

339

340 The taxonomy of *L. koalarum* strain UCD-LQP1 was confirmed in three ways. First, a
341 phylogenetic tree was built based on the 16S rRNA gene extracted from the new assembly. This
342 16S rRNA gene sequence was aligned with other closely related 16S rRNA gene sequences on
343 the RDP website where 16S rRNA gene sequences of type strains are curated and sequences of
344 the closest relatives of a taxon are usually readily available (Dunitz et al., 2015). The
345 phylogenetically closest sequence to *L. koalarum* strain UCD-LQP1 in the 16S rRNA gene tree
346 was one from *Lonepinella koalarum* Y17189 (Fig. 1). Second, a whole genome concatenated
347 gene marker tree was inferred using the Genome Taxonomy Database (GTDB), as well as using

348 PhyloSift, in parallel. In the GTDB tree, *L. koalarum* UCD-LQP1 was placed closest to
349 *Actinobacillus succinogenes* (GenBank accession number GCA_000017245.1). Note that as of
350 February 3, 2020, GTDB did not include any of the *L. koalarum* genome assemblies. In the
351 PhyloSift marker gene tree, all three *L. koalarum* assemblies clustered together, and *A.*
352 *succinogenes* was their phylogenetically closest neighbor (Fig. 2). Third, the average nucleotide
353 identity (ANI) between the genome of the *L. koalarum* type strain (DSM 10053; GenBank
354 accession number GCA_004339625.1) and the assembly of *L. koalarum* UCD-LQP1 was
355 estimated at 98.91 percent (standard deviation 0.17%). The ANI value between *L. koalarum*
356 UCD-LQP1 and GCA_004565475.1 was 98.99 percent (SD 0.15%) and the ANI value between
357 GCA_004339625.1 and GCA_004565475.1 was 99.99 percent (SD 0.08%). Both of these
358 genome assemblies are based on the type strain of *L. koalarum* that originated in 1995 (Osawa et
359 al., 1995). All three approaches confirmed the taxonomy of strain UCD-LQP1 as *Lonepinella*
360 *koalarum*. Interestingly, *A. succinogenes* (GenBank accession number GCA_000017245.1)
361 belongs now to a different taxonomic group based on GTDB taxonomy, namely *Basfia*
362 *succinogenes*. Parks et al. (2018), among others (e.g., Hug et al., 2016; Castelle & Banfield,
363 2018), have suggested relying on whole genome sequencing to reorganize the microbial tree of
364 life, which will result in a majority of changes in classification and naming, and ultimately
365 reflect a more accurate evolutionary relationship among groups (Parks et al., 2018).

366

367 There were no positive hits for any annotations associated with tannin degradation in the RAST
368 SEED viewer. This negative result is in contrast to the experimentally verified tannin-degrading
369 functions reported for this bacterium (Osawa et al., 1995). Moreover, tannic acid powder had
370 been used to prepare the culturing medium and was expected to help select for bacterial tannin
371 degraders. There are several potential explanations for the absence of any positive hits for
372 tannins in the RAST database including (1) the genes responsible for tannin degradation in the
373 assembly of *L. koalarum* UCD-LQP1 are not labeled as such, or (2) *L. koalarum* does not have
374 any tannin-degradation functionality. We thus carried out additional sequence-based analyses
375 searching for possible PCD degrading genes in the new assembly.

376

377 According to the annotation with PROKKA, there were 2,551 predicted genes and 2,479 protein
378 coding genes. In comparison, eggNOG predicted 2,370 protein coding genes. Neither annotation

379 included any genes annotated as “tannase”. However, among the eggNOG predictions, there
380 were 79 genes putatively involved in Class 1.11 Xenobiotics biodegradation and the degradation
381 of plant secondary metabolites (Table 2). There are 20 KEGG pathways included in this group.
382 We searched for all twenty pathways in the assembly of *L. koalarum* strain UCD-LQP1 and
383 found positive hits in 13 pathways (Table 2). Each hit represents a translated amino acid
384 sequence from the assembly of *L. koalarum* UCD-LQP1 that is encoded by an individual gene in
385 a pathway. The largest proportion of hits (n=15) comprised putative enzymes that are members
386 in this KEGG class, but do not fall into a particular pathway (KEGG pathway ko00983: Drug
387 metabolism - other enzymes). Potential tannin-degrading genes might be found in this group but
388 have not been labeled as tannase genes because their sequences are not similar enough to any
389 known tannase genes or because these tannase genes are not annotated in any database. The
390 second largest KEGG pathway was ko00362 benzoate degradation, followed by pathway
391 ko00980 metabolism of xenobiotics by Cytochrome P450 and pathway ko00625 chloroalkane
392 and chloroalkene degradation. KEGG pathways with fewer hits included the degradation
393 compounds such as aminobenzoate, xylene, naphthalene, dioxin, and chlorocyclohexane.
394 Mapping individual genes onto KEGG pathways revealed continuous degradation chains for the
395 following compounds: Azathioprine (pro-drug) to 6-Thioguanine (Supplementary Fig. S1);
396 Aminobenzoate degradation; *i.e.*, 4-Carboxy-2-hydroxymuconate semialdehyde to Pyruvate and
397 Oxaloacetate, which can then be fed into the citric acid cycle (Supplementary Fig. S2); 2-
398 Aminobenzene-sulfonate to Pyruvate, which, again, can be fed directly into Glycolysis or with
399 another enzyme that was present (1.2.1.10) can be converted into Acetaldehyde, then Acetyl-
400 CoA, and then fed into the Citrate cycle (Supplementary Fig. S2). In the group of xenobiotics
401 metabolized by cytochrome P450 there were seven complete chains (Supplementary Fig. S3):
402 degradation of (i) benzo(a)pyrene, (ii) Aflatoxin B1, (iii) 1-Nitronaphthalene, (iv) 1,1-Dichloro-
403 ethylene, (v) Trichloroethylene, (vi) Bromobenzene, and (vii) 1,2-Dibromoethane. All of these
404 complete, putative conversion chains present in *L. koalarum* might explain further how this
405 member of the koala gut microbiome contributes to koala gastro-physiology (see discussion
406 below). Amino acid sequences encoded by putative PCD degrading genes in *L. koalarum* strain
407 UCD-LQP1 can be downloaded from FigShare (Wilkins, 2020b). A table linking eggNOG
408 annotations to positions in individual assemblies and translated amino acid sequences can be

409 found in Supplementary Table S2. A complete table of all eggNOG annotations in the assembly
410 of *L. koalarum* strain UCD-LQP1 can be found in Supplementary Table S3.

411

412 *Eucalyptus* spp. leaves contain more than 100 different chemical compounds including
413 phenolics, terpenoids and lipids that are harmful for herbivores, even at low concentration
414 (Maghsoodlou et al., 2015). Koalas are highly specialized folivores feeding on these leaves. We
415 assumed that *L. koalarum* plays a beneficial role for koala hosts because some strains have
416 shown experimentally to be able to degrade tannins (Osawa, 1990; Osawa et al., 1995), and
417 tannic acid was used to isolate *L. koalarum* strain UCD-LQP1. Alas, we did not find any direct
418 evidence for tannase genes in the assembly of *L. koalarum* UCD-LQP1. However, genes
419 encoding several putative pathways involved in plant secondary metabolite degradation were
420 found in the assembly of *L. koalarum* UCD-LQP1. The predicted pathways included those for
421 degradation of compounds that had been extracted from *Eucalyptus* leaves (e.g., benzoate,
422 aminobenzoate, and chlorocyclohexane; Quinlivan et al., 2003; Marzoug et al., 2011; Sebei et
423 al., 2015; Maghsoodlou et al., 2015; Shiffman et al., 2017). Degradation of these PCDs might
424 explain the beneficial role that *L. koalarum* plays in the koala gut microbiome.

425

426 *Comparative genomics and unique genes in L. koalarum*

427 The GTDB tree clade used to extract related genomes of *L. koalarum* strain UCD-LQP1
428 consisted mostly of *Haemophilus* spp. (n = 28), followed by *Rodentibacter* spp. (n = 13),
429 *Pasteurella* spp. (n = 5), *Aggregibacter* spp. (n = 4), and seven other genera (Table S1). Whole
430 genome marker phylogenetic trees showed that not all genera were monophyletic. This can be
431 seen in Figure 2 in the way the coloring based on genus name does not group perfectly when taxa
432 are ordered according to their phylogenetic relationship. This was especially the case for
433 *Haemophilus* spp., which is shown in light purple. Some of the *Haemophilus* genomes were
434 grouped together, whereas others grouped with genomes labeled as *Pasteurella* spp.,
435 *Necropsobacter* spp. and *Avibacterium* spp. One species of *Rodentibacter* (*R. heylii*) was closest
436 to *Aggregatibacter* spp. (yellow and pink in Fig. 2). *Actinobacillus succinogenes* and
437 *Mannheimia succiniproducens* grouped with *Pasteurella* spp., while the former was the most
438 closely related non-*Lonepinella* genome to *L. koalarum* strain UCD-LQP1. Here it is worth
439 noting that both *A. succinogenes* and *M. succiniproducens* have been renamed in the new GTDB

440 taxonomy to *Basfia succinogenes*, most probably the most closely related taxon to *L. koalarum*
441 that has its genome sequenced to date. Twelve out of the 55 NCBI microbial genome assemblies
442 have different taxonomic names in the new GTDB taxonomy (Supplementary Table S1). For a
443 discussion of the re-organization and re-naming of the microbial tree of life based on whole
444 genome sequencing see above *Assembly taxonomy and gene annotation*. The whole genome
445 marker gene tree used to order genomes in Anvio's visualization can be downloaded from
446 FigShare (Wilkins, 2020c), as well as its corresponding amino acid alignment (Wilkins, 2020d).
447

448 Average nucleotide identities have been put forward as a measure of genomic relatedness among
449 bacteria that could help designate genera and be used besides the 16S rRNA gene as a taxonomic
450 marker (Barco et al., 2020). Moreover, it has been suggested to use an ANI threshold of larger
451 than 95% to delineate bacterial species (Goris et al., 2007). Based on this definition, the genomes
452 used for the comparative genomic analysis with *L. koalarum* are all distinct species (heatmap in
453 Fig. 2). We created a second heatmap visualizing genomic relatedness at the 70 % level
454 (Supplementary Fig. S4). This heatmap revealed several distinct clusters of closely related
455 genomes vs. singleton genomes (*i.e.*, taxa that did not group together with anything else at the 70
456 percent threshold): Cluster 1) *Aggregatibacter* spp., 2) first main *Haemophilus* spp. group, 3)
457 *Rodentibacter* spp., 4) second main *Haemophilus* spp. group, 5) *L. koalarum* genome assemblies,
458 and 6) two *Necropsobacter* spp. and another *Haemophilus* spp. Notably, *Rodentibacter heylii*, all
459 *Pasteurella* spp., and *Avibacterium paragallinarum* did not cluster with anything. The heatmap
460 is a way of visualizing sequence similarity groups and overall, it showed that the genera
461 *Haemophilus*, *Pasteurella* and *Rodentibacter* do not represent coherent groups of species or
462 genera. These three genera were found in several sub-groups (clusters in the ANI heatmap in
463 Supplementary Fig. S4) that have been described previously based on a much larger sample size
464 and a few marker genes (Naushad et al., 2015). Even some of the same singleton genomes were
465 reported as their own branches in previous phylogenetic trees (Christensen et al., 2003). *L.*
466 *koalarum* was placed in the middle of a group containing mostly *Haemophilus*, *Pasteurella* and
467 *Basfia* species. Pasteurellaceae, the single constituent family of the order Pasteurellales hosts a
468 diverse group of mostly pathogenic bacteria that had been assigned to this group based on
469 phenotypic traits, often related to their pathology, and GC content (Mannheim, Pohl &
470 Holländer, 1980). For example, the genus *Haemophilus* includes a plethora of taxa that cause

471 pneumonia and meningitis in humans, and *Pasteurella* have been associated with a range of
472 infectious diseases in cattle, fowl and pigs (Naushad et al., 2015). Moreover, since sequence-
473 based taxonomies have become more common, new genera have been created within each genus,
474 such as for example *Aggregatibacter* (Norskov-Lauritsen, 2006) or *Avibacterium* (Blackall et al.,
475 2005). We believe that a work-over of the evolutionary genetic relationship of the Pasteurellales
476 is overdue.

477

478 The proportion of gene clusters that were unique to the three *L. koalarum* genome assemblies,
479 relative to 55 of their most closely related genomes, was large relative to the size of genes that
480 were unique to other genera in Anvio's pangenome analysis (Fig. 2). There were 282 gene
481 clusters that could exclusively be found in the three *L. koalarum* genome assemblies. Among
482 them, there were 136 gene clusters with complete sequences and COG annotation
483 (Supplementary Table S4). There were 36 gene clusters unique to *L. koalarum* strain UCD-LQP1
484 and 19 of these had complete sequences and COG annotations (Supplementary Table S5).

485

486 Out of the 136 gene clusters with known COG functions that were unique to the three *L.*
487 *koalarum* genome assemblies, 22 different gene clusters fell into the COG category
488 'Carbohydrate metabolism/transport'. This was the largest category, followed by 'Inorganic ion
489 transport' (n = 15), 'Cell wall', 'Transcription', and 'Energy production' (n = 11, each), and
490 'Defense' (n = 7; Table 3 and Supplementary Table S4). The translated amino acid sequences for
491 these gene clusters, extracted from *L. koalarum* strain UCD-LQP1, can be found in
492 Supplementary Table S6.

493

494 Gene clusters in the category 'Carbohydrate metabolism and transport' are discussed in detail
495 below. It is worth mentioning that several putative components of the phosphotransferase system
496 were unique to *L. koalarum*. This system transports sugars into bacteria including glucose,
497 mannose, fructose, and cellobiose. It can differ among bacterial species, mirroring the most
498 suitable carbon sources available in the environment where a species evolved (Tchieu et al.,
499 2001). *L. koalarum* also stood out in terms of genes coding for cell wall components including
500 for example teichoic acid and other outer membrane proteins (Table 3 and Supplementary Table
501 S4). These outer membrane proteins are diverse and can significantly differ among bacterial

502 species (Schleifer & Kandler, 1972). A few other potentially unique gene clusters included genes
503 coding for type IV pilus assembly proteins for species-specific pili and fimbria (Proft & Baker,
504 2009); defense mechanisms, such as putative bacteriophage resistance proteins, phage repressor
505 proteins; and drug transport and efflux pumps. Several of these factors are characteristic for
506 pathogenic bacteria (Craig, Pique & Tainer, 2004). Here it is worth noting that a gram-negative
507 bacterium that was assigned to the genus *Lonepinella* based on 16S rRNA gene sequences
508 caused a human wound infection after a wildlife worker had been bitten by a koala (Sinclair et
509 al., 2019).

510

511 *Carbohydrate metabolism*

512 Since the majority of unique gene clusters in all three *L. koalarum* genome assemblies were
513 related to carbohydrate metabolism and transport, we decided to screen all three *L. koalarum*
514 assemblies for potential enzymes that assemble, modify, and breakdown oligo- and
515 polysaccharides. Using very stringent selection thresholds of the CAZy database where genes
516 coding for carbohydrate-active enzymes have to be identified by three different methods, we
517 found evidence for the presence of genes encoding 15 different glycoside hydrolase families,
518 three different carbohydrate esterase families, and nine different glycosyltransferase families
519 (Table 4). Note, gene families in *L. koalarum* are predicted to have these activities in
520 carbohydrate metabolism and transport based on characterized other members in the CAZy
521 database, but we do not provide experimental evidence that *L. koalarum* performs these
522 activities. All 28 identified CAZy gene families had also been annotated in the 2,370 eggNOG
523 annotations (Supplementary Table S3). Glycoside hydrolase families, GH2, GH31, GH32,
524 GH43, and GH77 were only found in the three *L. koalarum* genome assemblies relative to the
525 other taxa in the comparative genomic analysis (see also Table 3 and Supplementary Table S7).
526 These five glycoside hydrolases are responsible for the hydrolysis of glycosidic bonds. Notably,
527 when *Lonepinella koalarum* was isolated and described the first time as a phylogenetically and
528 phenotypically novel group within the family Pasteurellaceae, enzyme activities were determined
529 using commercially available oxidase/catalase tests as well as high-pressure liquid
530 chromatography (Osawa et al., 1995). The new taxon in 1995 (first described *L. koalarum*)
531 showed positive results for beta-galactosidase (putatively enzyme family GH2) and alpha-
532 amylase (putatively enzyme family GH77) and negative results for urease, arginine dihydrolase,

533 lysine decarboxylase, and tryptophane desaminase in congruence with the sequence-based results
534 here.

535

536 Genes coding for oligosaccharide-degrading enzymes in the families GH1, GH2, GH3, GH42,
537 and GH43 have also been found in another study that was investigating koala and wombat
538 metagenomes (Shiffman et al., 2017). Especially GH2, GH3 and GH43 were relatively common
539 in koala metagenomes, relative to wallaby foregut (Pope et al., 2010), cow rumen (Brulc et al.,
540 2009), and termite hindgut (He et al., 2013) metagenomes, where these enzymes had also been
541 characterized. These five glycoside hydrolase families comprise mostly oligosaccharide-
542 degrading enzymes (Allgaier et al., 2010); *i.e.*, they are able to break down a specific group of
543 monosaccharide sugars in other bacteria that had been characterized for the CAZy database.
544 However, presumably the major components of koala diet that are difficult to digest for the host
545 are plant secondary metabolites and plant cell walls in *Eucalyptus* leaves, and oligosaccharide-
546 degrading enzymes only play a significant role in a koala's diet after other enzymes have already
547 degraded cellulose in leaf plant cell walls (Moore et al., 2005). Oligosaccharides in *Eucalyptus*
548 leaves will be absorbed by the koala in the small intestine and only a small fraction enter the
549 caecum and colon. This means that the bacteria in the hindgut are most likely using their
550 metabolic pathways to process the products of the degradation of complex carbohydrates with
551 cross-feeding among microbiome members. The benefit of this activity to koala nutrition is not
552 well understood. Interestingly, among the genes that code for the three carbohydrate-active
553 enzyme families that were found exclusively in the assembly of *L. koalarum* strain UCD-LQP1,
554 two were actual lignocellulases; *i.e.*, microbial enzymes that hydrolyze the beta-1,4 linkages in
555 cellulose (Allgaier et al., 2010): Enzyme family GH42 and CE4. GH42 enzymes have mostly
556 been described in cellulose-degrading bacteria, archaea and fungi (Kosugi, Murashima & Doi,
557 2002; Shipkowski & Brenchley, 2006; Di Lauro et al., 2008). CE4 is a member of the
558 carbohydrate esterase family, which groups enzymes that catalyze the de-acetylation of plant cell
559 wall polysaccharides (Biely, 2012). Digestion of plant cell walls, (*i.e.*, cellulose, hemicellulose,
560 and lignin), could be a second explanation (besides PCD degradation) of how *L. koalarum* plays
561 a beneficial role in the koala gut microbiome.

562

563 *Antibiotic resistance genes*

564 Screening the three *L. koalarum* genome assemblies against the ResFinder database did not result
565 in any detection of antibiotic resistance variants. However, there were three hits in the CARD
566 database. First, all three *L. koalarum* assemblies contained a gene coding for a translated amino
567 acid variant at a specific position (SNP R234F) that had been shown to confer resistance to
568 pulvomycin in other bacterial species based on CARD predictions. Secondly, a variant was
569 found to be encoded in all three *L. koalarum* genome assemblies that had been described before
570 in *Haemophilus influenzae* mutant PBP3, conferring resistance to beta-lactam antibiotics
571 (cephalosporin, cephamycin, and penam) with SNPs D350N and S357N. The third result was an
572 amino acid position with reference to a protein homolog model in a *Klebsiella pneumoniae*
573 mutant, conferring resistance to the antibiotic efflux pump KpnH (including macrolide
574 antibiotics, fluoroquinolone, aminoglycoside, carbapenem, cephalosporin, penam, and penem).
575 These results are based on predictions from the CARD 2020 database. All three hits are
576 nucleotide sequences in the *L. koalarum* assemblies that are predicted to encode proteins that
577 showed the same amino acid variants as other bacterial species in the CARD database. We do
578 not know whether these variants confer antibiotic resistance in *L. koalarum*. Additional
579 experiments are necessary to confirm that these CARD predictions work for *L. koalarum*. The
580 corresponding nucleotide sequences and CARD output files are deposited on FigShare (UCD-
581 LQP1: Wilkins, 2020e; ATCC 700131: Wilkins, 2020f; and DSM 10053: Wilkins, 2020e).

582

583 *Recommendations for future koala management strategies*

584 In previous work, we identified *L. koalarum* as the most predictive taxon of koala survival
585 during antibiotic treatment and we suggested that this bacterium is important for koala health
586 (Dahlhausen et al., 2018). Here, we isolated a *L. koalarum* strain from the feces of a healthy
587 koala and sequenced and characterized its genome. We found several putative detoxification
588 pathways in *L. koalarum* strain UCD-LQP1 that could explain its potential beneficial role in the
589 koala gut for koala survival and fitness. Besides detoxification of plant secondary metabolites,
590 we found several putative genes involved in carbohydrate metabolism, particularly cellulose
591 degradation. Some of these genes were only found in *L. koalarum* assemblies and not in 55 of
592 their closely related genomes. Based on CARD predictions, the *L. koalarum* assemblies contain
593 some sequences that are similar to antibiotic resistance genes in other bacterial species. We
594 suggest confirming these antibiotic resistances in *L. koalarum* experimentally and testing the

595 efficiency of these antibiotic compounds against *Chlamydia* infections in koalas. In light of the
596 various threats that koalas face, from chlamydia infection to wildfires (Polkinghorne, Hanger &
597 Timms, 2013), and the growing interest in rescuing and treating them in sanctuaries and zoos, it
598 is important to identify beneficial members of their microbiome. This could (i) help decide
599 which antibiotic compounds to choose during chlamydia treatment in order to maximize
600 persistence of beneficial members in the koala gut microbiome, and (ii) guide the development
601 of probiotic cocktails during recovery (Jin Song et al., 2019).

602

603 **Acknowledgements**

604 We thank Céline Caseys ORCID: 0000-0003-4187-9018 for her idea to search eggNOG
605 annotations against KEGG Class 1.11 Xenobiotics biodegradation and metabolism pathways;
606 Chris Brown ORCID: 0000-0002-7758-6447 for his script to download assemblies in batch from
607 GenBank; Cassandra L. Ettinger ORCID: 0000-0001-7334-403X for valuable comments on the
608 panggenome analysis and help with revising the figures. We also thank Dr. Joseph Gillespie
609 ORCID: 0000-0002-5447-7264, Dr. Raphael Eisenhofer ORCID: 0000-0002-3843-0749 and two
610 anonymous reviewers for comments on the submitted manuscript.

611 **References**

- 612 Adamczyk B, Simon J, Kitunen V, Adamczyk S, Smolander A. 2017. Tannins and their complex
613 interaction with different organic nitrogen compounds and enzymes: Old paradigms versus
614 recent advances. *ChemistryOpen* 6:610-614. DOI: 10.1002/open.201700113.
- 615 Alcock BP, Raphenya AR, Lau TTY, Tsang KK, Bouchard M, Edalatmand A, Huynh W,
616 Nguyen A-LV, Cheng AA, Liu S, Min SY, Miroshnichenko A, Tran H-K, Werfalli RE,
617 Nasir JA, Oloni M, Speicher DJ, Florescu A, Singh B, Faltyn M, Hernandez-Koutoucheva
618 A, Sharma AN, Bordeleau E, Pawlowski AC, Zubyk HL, Dooley D, Griffiths E, Maguire F,
619 Winsor GL, Beiko RG, Brinkman FSL, Hsiao WWL, Domselaar GV, McArthur AG. 2020.
620 CARD 2020: Antibiotic resistome surveillance with the comprehensive antibiotic resistance
621 database. *Nucleic Acids Research* 48:D517–D525. DOI: 10.1093/nar/gkz935.
- 622 Alfano N, Courtiol A, Vielgrader H, Timms P, Roca AL, Greenwood AD. 2015. Variation in
623 koala microbiomes within and between individuals: Effect of body region and captivity
624 status. *Scientific Reports* 5:10189. DOI: 10.1038/srep10189.
- 625 Allgaier M, Reddy A, Park JI, Ivanova N, D'haeseleer P, Lowry S, Sapra R, Hazen TC,
626 Simmons BA, Vander Gheynst JS, Hugenholtz P. 2010. Targeted discovery of glycoside
627 hydrolases from a switchgrass-adapted compost community. *PLoS One* 5:e8812. DOI:
628 10.1371/journal.pone.0008812.
- 629 Altschul SF, Gish W, Miller W, Myers EW, Lipman DJ. 1990. Basic local alignment search tool.
630 *Journal of Molecular Biology* 215:403–410. DOI: 10.1016/S0022-2836(05)80360-2.
- 631 Aziz RK, Bartels D, Best AA, DeJongh M, Disz T, Edwards RA, Formsma K, Gerdes S, Glass
632 EM, Kubal M, Meyer F, Olsen GJ, Olson R, Osterman AL, Overbeek RA, McNeil LK,
633 Paarmann D, Paczian T, Parrello B, Pusch GD, Reich C, Stevens R, Vassieva O, Vonstein

- 634 V, Wilke A, Zagnitko O. 2008. The RAST Server: Rapid annotations using subsystems
635 technology. *BMC Genomics* 9:75. DOI: 10.1186/1471-2164-9-75.
- 636 Barco RA, Garrity GM, Scott JJ, Amend JP, Nealson KH, Emerson D. 2020. A genus definition
637 for bacteria and archaea based on a standard genome relatedness index. *mBio* 11. DOI:
638 10.1128/mBio.02475-19.
- 639 Biely P. 2012. Microbial carbohydrate esterases deacetylating plant polysaccharides.
640 *Biotechnology Advances* 30:1575–1588. DOI: 10.1016/j.biotechadv.2012.04.010.
- 641 Blackall PJ, Christensen H, Beckenham T, Blackall LL, Bisgaard M. 2005. Reclassification of
642 *Pasteurella gallinarum*, [*Haemophilus*] *paragallinarum*, *Pasteurella avium* and *Pasteurella*
643 *volantium* as *Avibacterium gallinarum* gen. nov., comb. nov., *Avibacterium paragallinarum*
644 comb. nov., *Avibacterium avium* comb. nov. and *Avibacterium volantium* comb. nov.
645 *International Journal of Systematic and Evolutionary Microbiology* 55:353–362.
- 646 Blyton MDJ, Soo RM, Whisson D, Marsh KJ, Pascoe J, Le Pla M, Foley M, Hugenholtz P,
647 Moore BD. 2019. Faecal inoculations alter the gastrointestinal microbiome and allow
648 dietary expansion in a wild specialist herbivore, the koala. *Animal Microbiome* 1:6. DOI:
649 10.1186/s42523-019-0008-0.
- 650 Brice KL, Trivedi P, Jeffries TC, Blyton MDJ, Mitchell C, Singh BK, Moore BD. 2019. The
651 koala (*Phascolarctos cinereus*) fecal microbiome differs with diet in a wild population.
652 *PeerJ* 7:e6534. DOI: 10.7717/peerj.6534.
- 653 Brulc JM, Antonopoulos DA, Miller MEB, Wilson MK, Yannarell AC, Dinsdale EA, Edwards
654 RE, Frank ED, Emerson JB, Wacklin P, Coutinho PM, Henrissat B, Nelson KE, White BA.
655 2009. Gene-centric metagenomics of the fiber-adherent bovine rumen microbiome reveals
656 forage specific glycoside hydrolases. *Proceedings of the National Academy of Sciences of*

- 657 *the United States of America* 106:1948–1953. DOI: 10.1073/pnas.0806191105.
- 658 Buchfink B, Xie C, Huson DH. 2015. Fast and sensitive protein alignment using DIAMOND.
659 *Nature Methods* 12:59–60. DOI: 10.1038/nmeth.3176.
- 660 Bushnell B. 2014. *BBMap: A fast, accurate, splice-aware aligner*. Lawrence Berkeley National
661 Lab. (LBNL), Berkeley, CA (United States).
- 662 Busk PK, Pilgaard B, Lezyk MJ, Meyer AS, Lange L. 2017. Homology to peptide pattern for
663 annotation of carbohydrate-active enzymes and prediction of function. *BMC Bioinformatics*
664 18:214. DOI: 10.1186/s12859-017-1625-9.
- 665 Callaghan J, McAlpine C, Mitchell D, Thompson J, Bowen M, Rhodes J, de Jong C,
666 Domalewski R, Scott A. 2011. Ranking and mapping koala habitat quality for conservation
667 planning on the basis of indirect evidence of tree-species use: a case study of Noosa Shire,
668 south-eastern Queensland. *Wildlife Research* 38:89. DOI: 10.1071/wr07177.
- 669 Cantarel BL, Coutinho PM, Rancurel C, Bernard T, Lombard V, Henrissat B. 2009. The
670 Carbohydrate-Active EnZymes database (CAZy): An expert resource for glycogenomics.
671 *Nucleic Acids Research* 37:D233–8. DOI: 10.1093/nar/gkn663.
- 672 Castelle CJ, Banfield JF. 2018. Major new microbial groups expand diversity and alter our
673 understanding of the tree of life. *Cell* 172:1181–1197. DOI: 10.1016/j.cell.2018.02.016.
- 674 Chaumeil PA, Hugenholtz P, Parks DH. 2018. GTDB-Tk: A toolkit to classify genomes with the
675 Genome Taxonomy Database. *Bioinformatics* 36:1925–1927. DOI:
676 10.1093/bioinformatics/btz848.
- 677 Christensen H, Bisgaard M, Bojesen AM, Muttters R, Olsen JE. 2003. Genetic relationships
678 among avian isolates classified as *Pasteurella haemolytica*, “*Actinobacillus salpingitidis*” or
679 *Pasteurella anatis* with proposal of *Gallibacterium anatis* gen. nov., comb. nov. and

- 680 description of additional genomospecies within *Gallibacterium* gen. nov. *International*
681 *Journal of Systematic and Evolutionary Microbiology* 53:275–287.
- 682 Cole JR, Wang Q, Fish JA, Chai B, McGarrell DM, Sun Y, Brown CT, Porras-Alfaro A, Kuske
683 CR, Tiedje JM. 2014. Ribosomal Database Project: Data and tools for high throughput
684 rRNA analysis. *Nucleic Acids Research* 42:D633–42. DOI: 10.1093/nar/gkt1244.
- 685 Craig L, Pique ME, Tainer JA. 2004. Type IV pilus structure and bacterial pathogenicity. *Nature*
686 *Reviews in Microbiology* 2:363–378. DOI: 10.1038/nrmicro885.
- 687 Dahlhausen KE, Doroud L, Firl AJ, Polkinghorne A, Eisen JA. 2018. Characterization of shifts
688 of koala (*Phascolarctos cinereus*) intestinal microbial communities associated with
689 antibiotic treatment. *PeerJ* 6:e4452. DOI: 10.7717/peerj.4452.
- 690 Darling AE, Jospin G, Lowe E, Matsen FA 4th, Bik HM, Eisen JA. 2014. PhyloSift:
691 Phylogenetic analysis of genomes and metagenomes. *PeerJ* 2:e243. DOI:
692 10.7717/peerj.243.
- 693 Delmont TO, Eren AM. 2018. Linking pangenomes and metagenomes: the *Prochlorococcus*
694 metapangenome. *PeerJ* 6:e4320. DOI: 10.7717/peerj.4320.
- 695 Desclozeaux M, Robbins A, Jelocnik M, Khan SA, Hanger J, Gerds V, Potter A, Polkinghorne
696 A, Timms P. 2017. Immunization of a wild koala population with a recombinant *Chlamydia*
697 *pecorum* Major Outer Membrane Protein (MOMP) or Polymorphic Membrane Protein
698 (PMP) based vaccine: New insights into immune response, protection and clearance. *PLoS*
699 *One* 12:e0178786. DOI: 10.1371/journal.pone.0178786.
- 700 Di Lauro B, Strazzulli A, Perugino G, La Cara F, Bedini E, Corsaro MM, Rossi M, Moracci M.
701 2008. Isolation and characterization of a new family 42 β -galactosidase from the
702 thermoacidophilic bacterium *Alicyclobacillus acidocaldarius*: Identification of the active

- 703 site residues. *Biochimica et Biophysica Acta (BBA) - Proteins and Proteomics* 1784:292–
704 301. DOI: 10.1016/j.bbapap.2007.10.013.
- 705 van Dongen S, Abreu-Goodger C. 2012. Using MCL to extract clusters from networks. *Methods*
706 *in Molecular Biology* 804:281–295. DOI: 10.1007/978-1-61779-361-5_15.
- 707 Dunitz MI, Lang JM, Jospin G, Darling AE, Eisen JA, Coil DA. 2015. Swabs to genomes: A
708 comprehensive workflow. *PeerJ* 3:e960. DOI: 10.7717/peerj.960.
- 709 Eddy SR. 1998. Profile hidden Markov models. *Bioinformatics* 14:755–763. DOI:
710 10.1093/bioinformatics/14.9.755.
- 711 Edgar RC. 2004. MUSCLE: A multiple sequence alignment method with reduced time and space
712 complexity. *BMC Bioinformatics* 5:113. DOI: 10.1186/1471-2105-5-113.
- 713 Eren AM, Esen ÖC, Quince C, Vineis JH, Morrison HG, Sogin ML, Delmont TO. 2015. Anvi'o:
714 An advanced analysis and visualization platform for 'omics data. *PeerJ* 3:e1319. DOI:
715 10.7717/peerj.1319.
- 716 Foley WJ, Lassak EV, Brophy J. 1987. Digestion and absorption of *Eucalyptus* essential oils in
717 greater glider (*Petauroide volans*) and brushtail possum (*Trichosurus vulpecula*). *Journal*
718 *of Chemical Ecology* 13:2115–2130. DOI: 10.1007/BF01012875.
- 719 Freeland WJ, Janzen DH. 1974. Strategies in herbivory by mammals: The role of plant
720 secondary compounds. *The American Naturalist* 108:269–289. DOI: 10.1086/282907.
- 721 Gleadow RM, Haburjak J, Dunn JE, Conn ME, Conn EE. 2008. Frequency and distribution of
722 cyanogenic glycosides in *Eucalyptus* L'Hérit. *Phytochemistry* 69:1870–1874. DOI:
723 10.1016/j.phytochem.2008.03.018.
- 724 Goel G, Puniya AK, Aguilar CN, Singh K. 2005. Interaction of gut microflora with tannins in
725 feeds. *Die Naturwissenschaften* 92:497–503. DOI: 10.1007/s00114-005-0040-7.

- 726 Goris J, Konstantinidis KT, Klappenbach JA, Coenye T, Vandamme P, Tiedje JM. 2007. DNA-
727 DNA hybridization values and their relationship to whole-genome sequence similarities.
728 *International Journal of Systematic and Evolutionary Microbiology* 57:81–91.
- 729 Gurevich A, Saveliev V, Vyahhi N, Tesler G. 2013. QUASt: Quality assessment tool for
730 genome assemblies. *Bioinformatics* 29:1072–1075. DOI: 10.1093/bioinformatics/btt086.
- 731 Hammer TJ, Bowers MD. 2015. Gut microbes may facilitate insect herbivory of chemically
732 defended plants. *Oecologia* 179:1–14. DOI: 10.1007/s00442-015-3327-1.
- 733 He S, Ivanova N, Kirton E, Allgaier M, Bergin C, Scheffrahn RH, Kyrpides NC, Warnecke F,
734 Tringe SG, Hugenholtz P. 2013. Comparative metagenomic and metatranscriptomic
735 analysis of hindgut paunch microbiota in wood- and dung-feeding higher termites. *PLoS*
736 *One* 8:e61126. DOI: 10.1371/journal.pone.0061126.
- 737 Higgins AL, Bercovitch FB, Tobey JR, Andrus CH. 2011. Dietary specialization and *Eucalyptus*
738 species preferences in Queensland koalas (*Phascolarctos cinereus*). *Zoo Biology* 30:52–58.
739 DOI: 10.1002/zoo.20312.
- 740 Hug LA, Baker BJ, Anantharaman K, Brown CT, Probst AJ, Castelle CJ, Butterfield CN,
741 Hermsdorf AW, Amano Y, Ise K, Suzuki Y, Dudek N, Relman DA, Finstad KM, Amundson
742 R, Thomas BC, Banfield JF. 2016. A new view of the tree of life. *Nature Microbiology*
743 1:16048. DOI: 10.1038/nmicrobiol.2016.48.
- 744 Hyatt D, Chen G-L, Locascio PF, Land ML, Larimer FW, Hauser LJ. 2010. Prodigal:
745 Prokaryotic gene recognition and translation initiation site identification. *BMC*
746 *Bioinformatics* 11:119. DOI: 10.1186/1471-2105-11-119.
- 747 Jensen LJ, Julien P, Kuhn M, von Mering C, Muller J, Doerks T, Bork P. 2008. eggNOG:
748 Automated construction and annotation of orthologous groups of genes. *Nucleic Acids*

749 *Research* 36:D250–4. DOI: 10.1093/nar/gkm796.

750 Jia B, Raphenya AR, Alcock B, Wagglechner N, Guo P, Tsang KK, Lago BA, Dave BM, Pereira
751 S, Sharma AN, Doshi S, Courtot M, Lo R, Williams LE, Frye JG, Elsayegh T, Sardar D,
752 Westman EL, Pawlowski AC, Johnson TA, Brinkman FSL, Wright GD, McArthur AG.
753 2017. CARD 2017: Expansion and model-centric curation of the comprehensive antibiotic
754 resistance database. *Nucleic Acids Research* 45:D566–D573. DOI: 10.1093/nar/gkw1004.

755 Jin Song S, Woodhams DC, Martino C, Allaband C, Mu A, Javorschi-Miller-Montgomery S,
756 Suchodolski JS, Knight R. 2019. Engineering the microbiome for animal health and
757 conservation. *Experimental Biology and Medicine* 244:494–504. DOI:
758 10.1177/1535370219830075.

759 Johnson RN, O’Meally D, Chen Z, Etherington GJ, Ho SYW, Nash WJ, Grueber CE, Cheng Y,
760 Whittington CM, Dennison S, Peel E, Haerty W, O’Neill RJ, Colgan D, Russell TL,
761 Alquezar-Planas DE, Attenbrow V, Bragg JG, Brandies PA, Chong AY-Y, Deakin JE, Di
762 Palma F, Duda Z, Eldridge MDB, Ewart KM, Hogg CJ, Frankham GJ, Georges A, Gillett
763 AK, Govendir M, Greenwood AD, Hayakawa T, Helgen KM, Hobbs M, Holleley CE,
764 Heider TN, Jones EA, King A, Madden D, Graves JAM, Morris KM, Neaves LE, Patel HR,
765 Polkinghorne A, Renfree MB, Robin C, Salinas R, Tsangaras K, Waters PD, Waters SA,
766 Wright B, Wilkins MR, Timms P, Belov K. 2018. Adaptation and conservation insights
767 from the koala genome. *Nature Genetics* 50:1102–1111. DOI: 10.1038/s41588-018-0153-5.

768 Jospin G. 2018. PhyloSift markers database. Figshare. DOI:
769 <https://doi.org/10.6084/m9.figshare.5755404.v4>

770 Kanehisa M, Goto S. 2000. KEGG: Kyoto encyclopedia of genes and genomes. *Nucleic Acids*
771 *Research* 28:27–30. DOI: 10.1093/nar/28.1.27.

- 772 Kohl KD, Weiss RB, Cox J, Dale C, Dearing MD. 2014. Gut microbes of mammalian herbivores
773 facilitate intake of plant toxins. *Ecology Letters* 17:1238-1246. DOI: 10.1111/ele.12329.
- 774 Kohl KD, Denise Dearing M. 2016. The woodrat gut microbiota as an experimental system for
775 understanding microbial metabolism of dietary toxins. *Frontiers in Microbiology* 7. DOI:
776 10.3389/fmicb.2016.01165.
- 777 Kohl KD, Stengel A, Denise Dearing M. 2016. Inoculation of tannin-degrading bacteria into
778 novel hosts increases performance on tannin-rich diets. *Environmental Microbiology*
779 18:1720–1729. DOI: 10.1111/1462-2920.12841.
- 780 Koren S, Walenz BP, Berlin K, Miller JR, Bergman NH, Phillippy AM. 2017. Canu: Scalable
781 and accurate long-read assembly via adaptive k-mer weighting and repeat separation.
782 *Genome Research* 27:722–736. DOI: 10.1101/gr.215087.116.
- 783 Kosugi A, Murashima K, Doi RH. 2002. Characterization of two noncellulosomal subunits,
784 ArfA and BgaA, from *Clostridium cellulovorans* that cooperate with the cellulosome in
785 plant cell wall degradation. *Journal of Bacteriology* 184:6859–6865. DOI:
786 10.1128/jb.184.24.6859-6865.2002.
- 787 Lawler IR, Foley WJ, Eschler BM. 2000. Foliar concentration of a single toxin creates habitat
788 patchiness for a marsupial folivore. *Ecology* 81:1327. DOI: 10.2307/177211.
- 789 Letunic I, Bork P. 2019. Interactive Tree Of Life (iTOL) v4: Recent updates and new
790 developments. *Nucleic Acids Research* 47:W256–W259. DOI: 10.1093/nar/gkz239.
- 791 Liu B, dos Santos BM, Kanagendran A, Neilson E, Niinemets Ü. 2019. Ozone and wounding
792 stresses differently alter the temporal variation in formylated phloroglucinols in *Eucalyptus*
793 globulus leave. *Metabolites* 9:46. DOI: 10.3390/metabo9030046.
- 794 Lombard V, Golaconda Ramulu H, Drula E, Coutinho PM, Henrissat B. 2014. The carbohydrate-

- 795 active enzymes database (CAZy) in 2013. *Nucleic Acids Research* 42:D490–5. DOI:
796 10.1093/nar/gkt1178.
- 797 Looft T, Levine UY, Stanton TB. 2013. *Cloacibacillus porcorum* sp. nov., a mucin-degrading
798 bacterium from the swine intestinal tract and emended description of the genus
799 *Cloacibacillus*. *International Journal of Systematic and Evolutionary Microbiology*
800 63:1960–1966. DOI: 10.1099/ijs.0.044719-0.
- 801 Madden T. 2003. *The BLAST Sequence Analysis Tool*. National Center for Biotechnology
802 Information (US).
- 803 Maghsoodlou MT, Kazemipoor N, Valizadeh J, Falak Nezhad Seifi M, Rahnesan N. 2015.
804 Essential oil composition of *Eucalyptus microtheca* and *Eucalyptus viminalis*. *Avicenna*
805 *Journal of Phytomedicine* 5:540–552.
- 806 Mannheim W, Pohl S, Holländer R. 1980. On the taxonomy of *Actinobacillus*, *Haemophilus*, and
807 *Pasteurella*: DNA base composition, respiratory quinones, and biochemical reactions of
808 representative collection cultures (author's transl). *Zentralblatt für Bakteriologie. I. Abt.*
809 *Originale. A: Medizinische Mikrobiologie, Infektionskrankheiten und Parasitologie*
810 246:512–540.
- 811 Marsh KJ, Foley WJ, Cowling A, Wallis IR. 2003. Differential susceptibility to *Eucalyptus*
812 secondary compounds explains feeding by the common ringtail (*Pseudocheirus peregrinus*)
813 and common brushtail possum (*Trichosurus vulpecula*). *Journal of Comparative*
814 *Physiology. B, Biochemical, Systemic, and Environmental Physiology* 173:69–78. DOI:
815 10.1007/s00360-002-0318-4.
- 816 Marzoug HNB, Romdhane M, Lebrihi A, Mathieu F, Couderc F, Abderraba M, Khouja ML,
817 Bouajila J. 2011. *Eucalyptus oleosa* essential oils: Chemical composition and antimicrobial

- 818 and antioxidant activities of the oils from different plant parts (stems, leaves, flowers and
819 fruits). *Molecules* 16:1695–1709. DOI: 10.3390/molecules16021695.
- 820 Miller MA, Pfeiffer W, Schwartz T. 2010. Creating the CIPRES Science Gateway for inference
821 of large phylogenetic trees. In: *2010 Gateway Computing Environments Workshop (GCE)*.
822 1–8. DOI: 10.1109/GCE.2010.5676129.
- 823 Moore BD, Foley WJ. 2005. Tree use by koalas in a chemically complex landscape. *Nature*
824 435:488–490. DOI: 10.1038/nature03551.
- 825 Moore BD, Foley WJ, Wallis IR, Cowling A, Handasyde KA. 2005. *Eucalyptus* foliar chemistry
826 explains selective feeding by koalas. *Biology Letters* 1:64–67. DOI:
827 10.1098/rsbl.2004.0255.
- 828 Naushad S, Adeolu M, Goel N, Khadka B, Al-Dahwi A, Gupta RS. 2015. Phylogenomic and
829 molecular demarcation of the core members of the polyphyletic Pasteurellaceae genera
830 *Actinobacillus*, *Haemophilus*, and *Pasteurella*. *International Journal of Genomics and*
831 *Proteomics* 2015. DOI: 10.1155/2015/198560.
- 832 Ngo S, Kong S, Kirlich A, McKinnon RA, Stupans I. 2000. Cytochrome P450 4A, peroxisomal
833 enzymes and nicotinamide cofactors in koala liver. *Comparative Biochemistry and*
834 *Physiology Part C: Pharmacology, Toxicology and Endocrinology* 127:327–334. DOI:
835 10.1016/s0742-8413(00)00160-2.
- 836 Norskov-Lauritsen N. 2006. Reclassification of *Actinobacillus actinomycetemcomitans*,
837 *Haemophilus aphrophilus*, *Haemophilus paraphrophilus* and *Haemophilus segnis* as
838 *Aggregatibacter actinomycetemcomitans* gen. nov., comb. nov., *Aggregatibacter*
839 *aphrophilus* comb. nov. and *Aggregatibacter segnis* comb. nov., and emended description
840 of *Aggregatibacter aphrophilus* to include V factor-dependent and V factor-independent

- 841 isolates. *International Journal of Systematic and Evolutionary Microbiology* 56:2135–2146.
842 DOI: 10.1099/ijs.0.64207-0.
- 843 Nyari S, Khan SA, Rawlinson G, Waugh CA, Potter A, Gerdt V, Timms P. 2018. Vaccination
844 of koalas (*Phascolarctos cinereus*) against *Chlamydia pecorum* using synthetic peptides
845 derived from the major outer membrane protein. *PLoS One* 13:e0200112. DOI:
846 10.1371/journal.pone.0200112.
- 847 Osawa R. 1990. Formation of a clear zone on tannin-treated brain heart infusion agar by a
848 *Streptococcus* sp. isolated from feces of koalas. *Applied and Environmental Microbiology*
849 56:829–831.
- 850 Osawa R. 1992. Tannin-protein complex-degrading *Enterobacteria* isolated from the alimentary
851 tract of koalas and a selective medium for their enumeration. *Applied and Environmental*
852 *Microbiology* 58:1754–1759.
- 853 Osawa R, Bird PS, Harbrow DJ, Ogimoto K, Seymour GJ. 1993. Microbiological studies of the
854 intestinal microflora of the koala, *Phascolarctos cinereus*: Colonization of the cecal wall by
855 tannin-protein-complex-degrading *Enterobacteria*. *Australian Journal of Zoology* 41:599.
856 DOI: 10.1071/zo9930599.
- 857 Osawa R, Rainey F, Fujisawa T, Lang E, Busse HJ, Walsh TP, Stackebrandt E. 1995.
858 *Lonepinella koalarum* gen. nov., sp. nov., a new tannin-protein complex degrading
859 bacterium. *Systematic and Applied Microbiology* 18:368–373. DOI: 10.1016/s0723-
860 2020(11)80430-3.
- 861 Overbeek R, Olson R, Pusch GD, Olsen GJ, Davis JJ, Disz T, Edwards RA, Gerdes S, Parrello
862 B, Shukla M, Vonstein V, Wattam AR, Xia F, Stevens R. 2014. The SEED and the Rapid
863 Annotation of microbial genomes using Subsystems Technology (RAST). *Nucleic Acids*

- 864 *Research* 42:D206–14. DOI: 10.1093/nar/gkt1226.
- 865 Parks DH, Chuvochina M, Waite DW, Rinke C, Skarshewski A, Chaumeil P-A, Hugenholtz P.
866 2018. A standardized bacterial taxonomy based on genome phylogeny substantially revises
867 the tree of life. *Nature Biotechnology* 36:996–1004. DOI: 10.1038/nbt.4229.
- 868 Parks DH, Imelfort M, Skennerton CT, Hugenholtz P, Tyson GW. 2015. CheckM: Assessing the
869 quality of microbial genomes recovered from isolates, single cells, and metagenomes.
870 *Genome Research* 25:1043–1055. DOI: 10.1101/gr.186072.114.
- 871 Polkinghorne A, Hanger J, Timms P. 2013. Recent advances in understanding the biology,
872 epidemiology and control of chlamydial infections in koalas. *Veterinary Microbiology*
873 165:214–223. DOI: 10.1016/j.vetmic.2013.02.026.
- 874 Pope PB, Denman SE, Jones M, Tringe SG, Barry K, Malfatti SA, McHardy AC, Cheng J-. F,
875 Hugenholtz P, McSweeney CS, Morrison M. 2010. Adaptation to herbivory by the Tamar
876 wallaby includes bacterial and glycoside hydrolase profiles different from other herbivores.
877 *Proceedings of the National Academy of Sciences* 107:14793–14798. DOI:
878 10.1073/pnas.1005297107.
- 879 Price MN, Dehal PS, Arkin AP. 2009. FastTree: Computing large minimum evolution trees with
880 profiles instead of a distance matrix. *Molecular Biology and Evolution* 26:1641–1650. DOI:
881 10.1093/molbev/msp077.
- 882 Pritchard L, Glover RH, Humphris S, Elphinstone JG, Toth IK. 2016. Genomics and taxonomy
883 in diagnostics for food security: soft-rotting enterobacterial plant pathogens. *Analytical*
884 *Methods* 8:12–24. DOI: 10.1039/C5AY02550H.
- 885 Proft T, Baker EN. 2009. Pili in Gram-negative and Gram-positive bacteria — structure,
886 assembly and their role in disease. *Cellular and Molecular Life Sciences* 66:613–635. DOI:

- 887 10.1007/s00018-008-8477-4.
- 888 Quinlivan EP, Roje S, Basset G, Shachar-Hill Y, Gregory JF 3rd, Hanson AD. 2003. The folate
889 precursor p-aminobenzoate is reversibly converted to its glucose ester in the plant cytosol.
890 *The Journal of Biological Chemistry* 278:20731–20737. DOI: 10.1074/jbc.M302894200.
- 891 R Development Core Team. 2013. *A language and environment for statistical computing*. R
892 *Foundation for Statistical Computing, Vienna, Austria*.
- 893 Schleifer KH, Kandler O. 1972. Peptidoglycan types of bacterial cell walls and their taxonomic
894 implications. *Bacteriological Reviews* 36:407.
- 895 Sebei K, Sakouhi F, Herchi W, Khouja ML, Boukhchina S. 2015. Chemical composition and
896 antibacterial activities of seven *Eucalyptus* species essential oils leaves. *Biological*
897 *Research* 48:7. DOI: 10.1186/0717-6287-48-7.
- 898 Seemann T. 2014. Prokka: Rapid prokaryotic genome annotation. *Bioinformatics* 30:2068–2069.
899 DOI: 10.1093/bioinformatics/btu153.
- 900 Shiffman ME, Soo RM, Dennis PG, Morrison M, Tyson GW, Hugenholtz P. 2017. Gene and
901 genome-centric analyses of koala and wombat fecal microbiomes point to metabolic
902 specialization for digestion. *PeerJ* 5:e4075. DOI: 10.7717/peerj.4075.
- 903 Shipkowski S, Brenchley JE. 2006. Bioinformatic, genetic, and biochemical evidence that some
904 glycoside hydrolase family 42 beta-galactosidases are arabinogalactan type I oligomer
905 hydrolases. *Applied and Environmental Microbiology* 72:7730–7738. DOI:
906 10.1128/AEM.01306-06.
- 907 Sinclair HA, Chapman P, Omaleki L, Bergh H, Turni C, Blackall P, Papacostas L, Braslins P,
908 Sowden D, Nimmo GR. 2019. Identification of *Lonepinella* sp. in koala bite wound
909 infections, Queensland, Australia. *Emerging Infectious Diseases* 25:153–156. DOI:

- 910 10.3201/eid2501.171359.
- 911 SNPsaurus | GENOMES to GENOTYPES. Available at <https://www.snpsaurus.com> (accessed
912 August 20, 2019).
- 913 Stackebrandt E, Goodfellow M. 1991. *Nucleic Acid Techniques in Bacterial Systematics*. John
914 Wiley & Son Ltd.
- 915 Stucky BJ. 2012. SeqTrace: A graphical tool for rapidly processing DNA sequencing
916 chromatograms. *Journal of Biomolecular Techniques: JBT* 23:90–93. DOI: 10.7171/jbt.12-
917 2303-004.
- 918 Tchieu JH, Norris V, Edwards JS, Saier MH Jr. 2001. The complete phosphotransferase system
919 in *Escherichia coli*. *Journal of Molecular Microbiology and Biotechnology* 3:329–346.
- 920 Turner S, Pryer KM, Miao VP, Palmer JD. 1999. Investigating deep phylogenetic relationships
921 among cyanobacteria and plastids by small subunit rRNA sequence analysis. *The Journal of*
922 *Eukaryotic Microbiology* 46:327–338. DOI: 10.1111/j.1550-7408.1999.tb04612.x.
- 923 Waterman PG, Mbi CN, McKey DB, Stephen Gartlan J. 1980. African rainforest vegetation and
924 rumen microbes: Phenolic compounds and nutrients as correlates of digestibility. *Oecologia*
925 47:22–33. DOI: 10.1007/bf00541771.
- 926 Waugh C, Khan SA, Carver S, Hanger J, Loader J, Polkinghorne A, Beagley K, Timms P. 2016.
927 A prototype recombinant-protein based *Chlamydia pecorum* vaccine results in reduced
928 Chlamydial burden and less clinical disease in free-ranging koalas (*Phascolarctos*
929 *cinereus*). *PLoS One* 11:e0146934. DOI: 10.1371/journal.pone.0146934.
- 930 Wick RR, Judd LM, Gorrie CL, Holt KE. 2017. Unicycler: Resolving bacterial genome
931 assemblies from short and long sequencing reads. *PLoS Computational Biology*
932 8:e1005595. DOI: 10.1371/journal.pcbi.1005595.

- 933 Wilkins LGE. 2020a. *Notebook Lonopinella koalarum comparative genomic analysis*. Figshare.
934 DOI: <https://doi.org/10.6084/m9.figshare.11678262.v1>
- 935 Wilkins LGE. 2020b. Putative amino acid sequences involved in xenobiotics biodegradation and
936 metabolism. Figshare. DOI: <https://doi.org/10.6084/m9.figshare.11719278.v1>
- 937 Wilkins LGE. 2020c. Tree file RAxML to order genomes in Anvi'o. Figshare. DOI:
938 <https://doi.org/10.6084/m9.figshare.11719338.v1>
- 939 Wilkins LGE. 2020d. Amino acid alignment from PhyloSift to order genomes in Anvi'o.
940 Figshare. DOI: <https://doi.org/10.6084/m9.figshare.11719326.v1>
- 941 Wilkins LGE. 2020e. Antibiotic resistance genes in GCA_004339625; *Lonopinella koalarum*.
942 Figshare. DOI: <https://doi.org/10.6084/m9.figshare.11760249.v1>
- 943 Wilkins LGE. 2020f. Antibiotic resistance genes in GCA_004565475; *Lonopinella koalarum*.
944 Figshare. DOI: <https://doi.org/10.6084/m9.figshare.11760219.v2>
- 945 Wilkins LGE. 2020g. Anvi'o genomes database for *Lonopinella koalarum*. Figshare. DOI:
946 <https://doi.org/10.6084/m9.figshare.11760285.v1>
- 947 Wilkins LGE. 2020h. Anvi'o profile for *Lonopinella koalarum*. Figshare. DOI:
948 <https://doi.org/10.6084/m9.figshare.11760324.v1>
- 949 Wilkins LGE, Coil DA. 2020a. 16S rRNA gene based alignment. Figshare. DOI:
950 <https://doi.org/10.6084/m9.figshare.11678265.v1>
- 951 Wilkins LGE, Coil DA. 2020b. 16S rRNA gene phylogenetic tree. Figshare. DOI:
952 <https://doi.org/10.6084/m9.figshare.11678259.v1>
- 953 Wilkins LGE, Ettinger CL, Jospin G, Eisen JA. 2019. Metagenome-assembled genomes provide
954 new insight into the microbial diversity of two thermal pools in Kamchatka, Russia.
955 *Scientific Reports* 9:3059. DOI: 10.1038/s41598-019-39576-6.

- 956 Wilkins LGE, Jospin G. 2020. Contig 9 - potential *Lonepinella koalarum* plasmid. Figshare.
957 DOI: <https://doi.org/10.6084/m9.figshare.11717895.v1>
- 958 Yin Y, Mao X, Yang J, Chen X, Mao F, Xu Y. 2012. dbCAN: A web resource for automated
959 carbohydrate-active enzyme annotation. *Nucleic Acids Research* 40:W445–51. DOI:
960 10.1093/nar/gks479.
- 961 Zankari E, Hasman H, Cosentino S, Vestergaard M, Rasmussen S, Lund O, Aarestrup FM,
962 Larsen MV. 2012. Identification of acquired antimicrobial resistance genes. *Journal of*
963 *Antimicrobial Chemotherapy* 67:2640–2644. DOI: 10.1093/jac/dks261.

Figure 1

16S rRNA gene phylogenetic placement of *Lonepinella koalarum* strain UCD-LQP1

The 16S rRNA gene was extracted from the *L. koalarum* genome assembly by searching for 'ssu rRNA' in the RAST function search of the SEED genome browser (Aziz et al., 2008; Overbeek et al., 2014). Included are all known 16S rRNA sequences in the Pasteurellaceae family and one outgroup, *Agarivoran* spp. Nodes and tip labels are colored corresponding to the Anvi'o profile in Figure 2; *i.e.*, red: *Lonepinella koalarum* (Unicycler: assembly of *L. koalarum* strain UCD-LQP1, in bold and marked with a star), dark purple: *Pasteurella* spp., light purple: *Haemophilus* spp., orange: *Actinobacillus* spp., pink: *Aggregatibacter* spp., and green: *Mannheimia* spp. Black are genera that were not used in Figure 2, and brown depicts the outgroup *Agarivoran* spp.

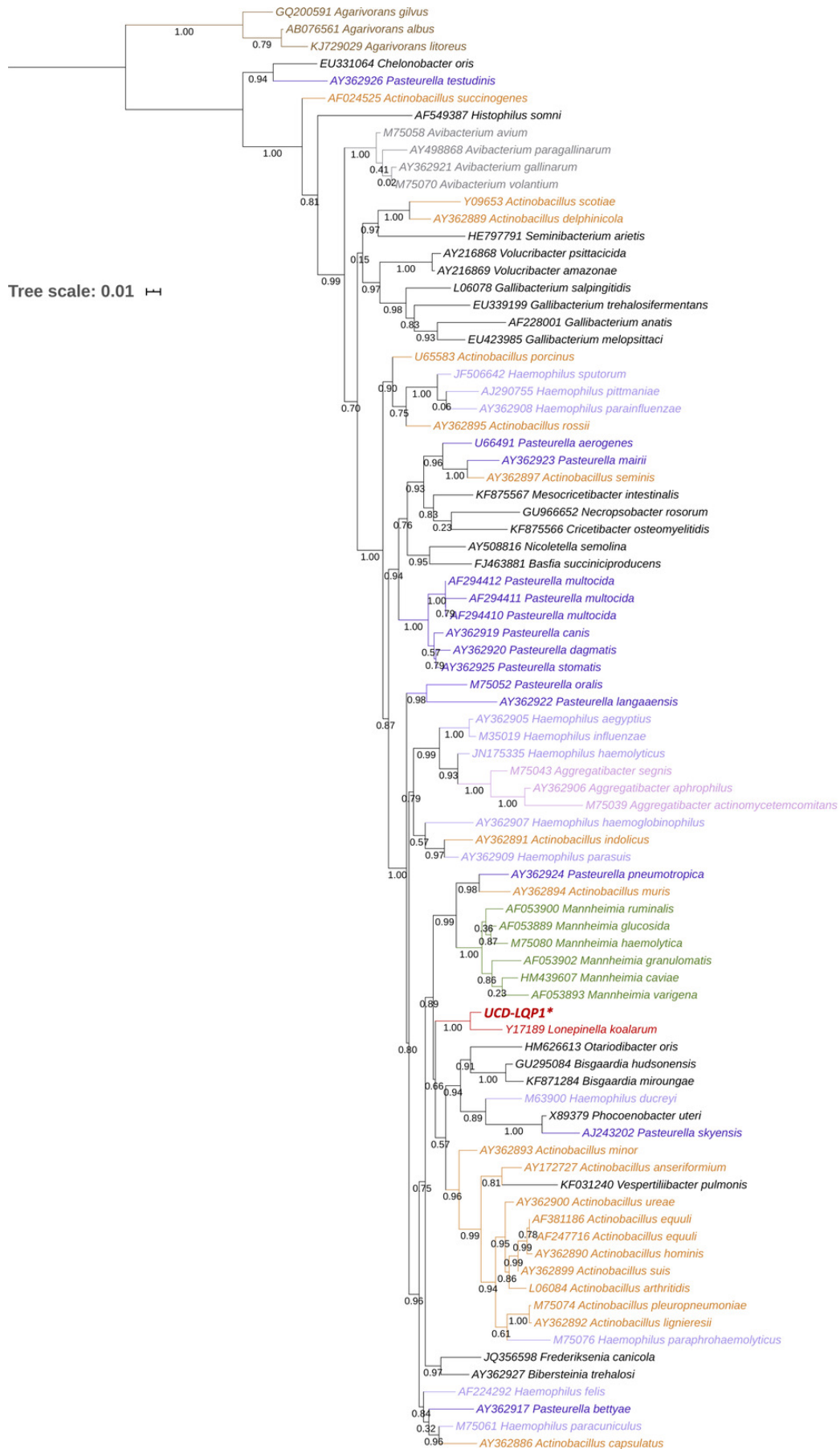


Figure 2

Pangenome comparison of *L. koalarum* strain UCD-LQP1 and 57 of its most closely related, publicly available genomes

This figure was generated from the microbial pangenomic analysis in Anvi'o version 5.5 where each ring represents an individual genome assembly. After ordering all taxa according to a genomic marker gene tree, genomes were colored following NCBI taxonomy (red: *Lonepinella koalarum*, dark purple: *Pasteurella* spp., light purple: *Haemophilus* spp., pink: *Aggregatibacter* spp., green: *Mannheimia* spp., light green: *Avibacterium paragallinarum*, grey: *Necropsobacter* spp., and yellow: *Rodentibacter* spp. Note, *Actinobacillus* spp. was colored in green here and not orange as in Fig. 1 to show its relation to *Mannheimia* spp. According to GTDB taxonomy, those two genomes are now *Basfia* species. See Discussion section). Each wedge represents a gene cluster. Gene clusters were grouped into mostly shared, shared, private, and in red: exclusively found in *Lonepinella koalarum* genome assemblies: 'LK', and exclusively found in *L. koalarum* strain UCD-LQP1. The gene marker tree was created in PhyloSift version 1.0.1 (Darling et al., 2014) with its updated markers database (version 4, posted on 12th of February 2018; Jospin, 2018) for the alignment and RAXML version 8.2.10 on the CIPRES web server for the tree inference (Miller, Pfeiffer & Schwartz, 2010). Gene clusters were ordered based on presence/absence. Also shown is GC content in light brown, number of genes per kilo base pairs in light grey, number of gene clusters in dark grey, and number of singleton gene clusters in orange, for each assembly, respectively. The heatmap shows ANI (Average nucleotide identity) values > 95%. The ANI heatmap is aligned with the Anvi'o profile, leading to the genome IDs on the y-axis. The Anvi'o database (Wilkins, 2020g) and profile (Wilkins, 2020h) are accessible on FigShare.

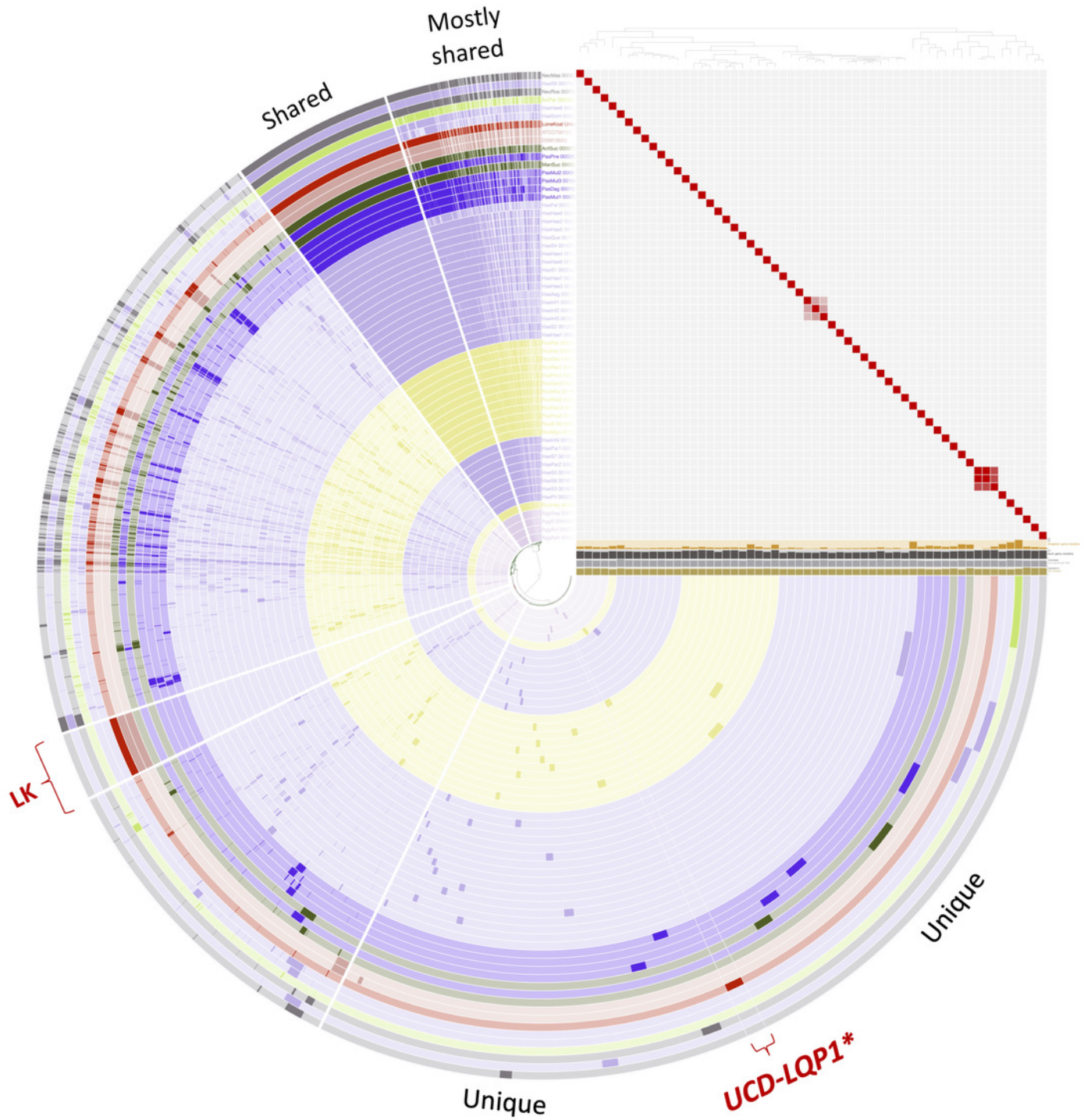


Table 1 (on next page)

Lonepinella koalarum strain UCD-LQP1 assembly statistics

Completeness and contamination were determined with CheckM version 1.0.8 (Parks et al., 2015); number of contigs, total length, GC%, N50, N75, L50, and L75 were determined with QUAST (Quality Assessment Tool for Genome Assemblies) (Gurevich et al., 2013); number of predicted genes and number of protein coding genes were determined with PROKKA version 1.12 (Seemann, 2014).

1

Statistic	Value
Completeness	99.205 %
Contamination	0.705 %
Number of Contigs	29
Total Length	2,608,483 bp
GC%	39.02
N50	2,299,135 bp
N75	2,299,135 bp
L50	1
L75	1
Number of Predicted Genes	2,551
Number of Protein Coding Genes	2,479

2

Table 2 (on next page)

KEGG pathways involved in xenobiotics biodegradation and metabolism

Twenty KEGG pathways known to play a role in plant secondary metabolite degradation (Kanehisa & Goto, 2000) were searched in the eggNOG annotations of *Lonepinella koalarum* strain UCD-LQP1 (Hits). The translated amino acid sequences encoded by putative genes in *L. koalarum* can be downloaded from FigShare (Wilkins, 2020b).

KEGG: Xenobiotics biodegradation and metabolism

Pathway	Hits	KEGG ID
Drug metabolism - Other enzymes	15	ko00983
Benzoate degradation	14	ko00362
Metabolism of xenobiotics by Cytochrome P450	9	ko00980
Chloroalkane and chloroalkene degradation	8	ko00625
Aminobenzoate degradation	6	ko00627
Xylene degradation	6	ko00622
Naphthalene degradation	6	ko00626
Dioxin degradation	5	ko00621
Chlorocyclohexane and chlorobenzene degradation	3	ko00361
Toluene degradation	2	ko00623
Nitrotoluene degradation	2	ko00633
Styrene degradation	2	ko00643
Fluorobenzoate degradation	1	ko00364
Ethylbenzene degradation	0	ko00642
Atrazine degradation	0	ko00791
Caprolactam degradation	0	ko00930
Bisphenol degradation	0	ko00363
Polycyclic aromatic hydrocarbon degradation	0	ko00624
Furfural degradation	0	ko00365
Steroid degradation	0	ko00984

1

Table 3(on next page)

Unique gene clusters and their COG IDs in three *Lonepinella koalarum* genome assemblies

A comparative genomic analysis was performed in Anvi'o version 5.5 (Eren et al., 2015) to compare three publicly available *Lonepinella koalarum* genome assemblies to 55 closely related genomes. Gene clusters that could only be found in *L. koalarum* relative to the rest were filtered out and annotated with COG (Clusters of Orthologous Groups). Carbohydrate-active enzymes are shaded in grey. Only a subset of COG categories are shown; G: 'Carbohydrate metabolism/transport', M: 'Cell wall', H: 'Coenzyme metabolism', V: 'Defense', C: 'Energy production', W: 'Extracellular', P: 'Inorganic ion transport', X: 'Prophages and Transposon', L: 'Replication and Repair'. The complete list of unique gene clusters and their translated amino acid sequence in *L. koalarum* can be found in Supplementary Tables S4-S6.

Gene ID	COG ID	COG Function	COG Category
1408	COG1501	Alpha-glucosidase, glycosyl hydrolase family GH31	G
1251	COG3534	Alpha-L-arabinofuranosidase Alpha-L-arabinofuranosidase	G
1643	COG2723	Beta-galactosidase	G
1513	COG0129	Dihydroxyacid dehydratase/phosphogluconate dehydratase	G
1404	COG1349	DNA-binding transcriptional regulator of sugar metabolism, DeoR/GlpR family	G
1410	COG2017	Galactose mutarotase or related enzyme	G
1204	COG2220	L-ascorbate metabolism protein UlaG, beta-lactamase superfamily	G
1409	COG2942	Mannose or cellobiose epimerase, N-acyl-D-glucosamine 2-epimerase family	G
1250	COG2211	Na ⁺ /melibiose symporter or related transporter	G
1642	COG1472	Periplasmic beta-glucosidase and related glycosidases	G
810	COG1447	Phosphotransferase system cellobiose-specific component IIA	G
812	COG1440	Phosphotransferase system cellobiose-specific component IIB	G
808	COG1455	Phosphotransferase system cellobiose-specific component IIC	G
2231	COG1263	Phosphotransferase system IIC components, glucose-specific	G
811	COG1762	Phosphotransferase system mannitol/fructose-specific IIA domain (Ntr-type)	G
2230	COG1621	Sucrose-6-phosphate hydrolase SacC, GH32 family	G
1372	COG0524	Sugar or nucleoside kinase, ribokinase family	G
1407	COG3684	Tagatose-1,6-bisphosphate aldolase	G
1729	COG3711	Transcriptional antiterminator Mannitol/fructose-specific phosphotransferase system, IIA domain	G
1402	COG1593	TRAP-type C4-dicarboxylate transport system, large permease component	G
1401	COG1638	TRAP-type C4-dicarboxylate transport system, periplasmic component	G
1403	COG3090	TRAP-type C4-dicarboxylate transport system, small permease component	G
1023	COG0859	ADP-heptose:LPS heptosyltransferase	M
815	COG3659	Carbohydrate-selective porin OprB	M
264	COG3765	LPS O-antigen chain length determinant protein, WzzB/FepE family	M
1623	COG1388	LysM repeat	M
2084	COG2244	Membrane protein involved in the export of O-antigen and teichoic acid	M
489	COG0451	Nucleoside-diphosphate-sugar epimerase	M
1468	COG3307	O-antigen ligase	M
221	COG3203	Outer membrane protein (porin)	M
557	COG1538	Outer membrane protein TolC	M
199	COG0810	Periplasmic protein TonB, links inner and outer membranes	M
1187	COG2843	Poly-gamma-glutamate biosynthesis protein CapA/YwtB (capsule formation), metallophosphatase superfamily	M
495	COG0043	3-polyprenyl-4-hydroxybenzoate decarboxylase	H
1371	COG3201	Nicotinamide riboside transporter PnuC	H
413	COG4206	Outer membrane cobalamin receptor protein	H
817	COG1477	Thiamine biosynthesis lipoprotein ApbE	H
2228	COG2226	Ubiquinone/menaquinone biosynthesis C-methylase UbiE	H
2071	COG1401	5-methylcytosine-specific restriction endonuclease McrBC, GTP-binding regulatory subunit McrB	V
1160	COG1132	ABC-type multidrug transport system, ATPase and permease component	V
1058	COG4823	Abortive infection bacteriophage resistance protein	V
1573	COG0251	Enamine deaminase RidA, house cleaning of reactive enamine intermediates	V

1669	COG2337	mRNA-degrading endonuclease, toxin component of the MazEF toxin-antitoxin module	V
2012	COG0845	Multidrug efflux pump subunit AcrA (membrane-fusion protein)	V
432	COG3093	Plasmid maintenance system antidote protein VapI, contains XRE-type HTH domain	V
1138	COG2828	2-Methylnaconitate cis-trans-isomerase PrpF (2-methyl citrate pathway)	C
9	COG1048	Aconitase A	C
311	COG1454	Alcohol dehydrogenase, class IV	C
1134	COG3312	FoF1-type ATP synthase assembly protein I	C
2130	COG0435	Glutathionyl-hydroquinone reductase	C
763	COG0371	Glycerol dehydrogenase or related enzyme, iron-containing ADH family	C
1584	COG0778	Nitroreductase	C
816	COG1053	Succinate dehydrogenase/fumarate reductase, flavoprotein subunit	C
514	COG4972	Tfp pilus assembly protein, ATPase PilM	W
2098	COG1116	ABC-type nitrate/sulfonate/bicarbonate transport system, ATPase component	P
2097	COG0715	ABC-type nitrate/sulfonate/bicarbonate transport system, periplasmic component	P
592	COG0600	ABC-type nitrate/sulfonate/bicarbonate transport system, permease component	P
818	COG2807	Cyanate permease	P
2005	COG2382	Enterochelin esterase or related enzyme	P
234	COG3301	Formate-dependent nitrite reductase, membrane component NrfD	P
365	COG3230	Heme oxygenase	P
1053	COG0672	High-affinity Fe ²⁺ /Pb ²⁺ permease	P
1051	COG2822	Iron uptake system EfeUOB, periplasmic (or lipoprotein) component EfeO/EfeM	P
28	COG2375	NADPH-dependent ferric siderophore reductase, contains FAD-binding and SIP domains	P
1158	COG2223	Nitrate/nitrite transporter NarK	P
1209	COG2223	Nitrate/nitrite transporter NarK	P
1089	COG4771	Outer membrane receptor for ferrienterochelin and colicins	P
1052	COG2837	Periplasmic deferrochelate/oxidase EfeB	P
310	COG0659	Sulfate permease or related transporter, MFS superfamily	P
631	COG4388	Mu-like prophage I protein	X
662	COG2932	Phage repressor protein C, contains Cro/C1-type HTH and peptisase s24 domains	X
2183	COG5412	Phage-related protein	X
1780	COG1943	REP element-mobilizing transposase RayT	X
1057	COG2189	Adenine specific DNA methylase Mod	L
48	COG1074	ATP-dependent exoDNase (exonuclease V) beta subunit (contains helicase and exonuclease domains)	L
47	COG0507	ATP-dependent exoDNase (exonuclease V), alpha subunit, helicase superfamily I	L
2035	COG3057	Negative regulator of replication initiation	L

Table 4(on next page)

Putative carbohydrate-active enzymes (CAZy) found in *Lonepinella koalarum* genome assemblies

Genes coding for putative carbohydrate-active enzymes (CAZy enzymes) that were only found in *Lonepinella koalarum* relative to 55 closely related genomes are shaded in grey (corresponding to Table 3), and CAZy enzymes that were only found in the assembly of *L. koalarum* UCD-LQP1 alone are presented in bold. The position of genes potentially coding for these enzymes in the assembly of *L. koalarum* UCD-LQP1 are shown as well. See Material and methods section for details on how assemblies were screened for CAZy enzymes. Positions of these genes in *L. koalarum* genome assemblies ATCC 700131 and DSM 10053 are shown in Supplementary Table S7.

CAZy	Enzyme	LK position
GH1	β -Glycosidase; membrane-bound lytic transglycosylase A (MltA)	1_1622
GH2	β -Galactosidase	1_1329
GH3	Glycoside hydrolase Family 3	1_1536
GH4	α - and β -Glycosidases	1_1355
GH13	Major glycoside hydrolase family acting on substrates containing α -glucoside linkages	1_1263
GH20	Retaining glycoside hydrolases	1_757
GH23	Lytic transglycosylases of GH23	1_1073
GH31	α -Glucosidases	1_1388
GH32	Inverting sucrose; invertase	2_66
GH33	Glycoside hydrolase family 33	1_1214
GH42	Plant cell wall degradation	1_1367
GH43	α -L-Arabinofuranosidase and β -D-xylosidase activity	1_1369
GH77	α -Amylase	3_8
GH102	Lytic transglycosylases	1_346
GH103	Lytic transglycosylase B (MltB)	2_81
CE4	Deacylation of polysaccharides	1_760
CE9	Deacetylation of N-acetylglucosamine-6-phosphate	1_1583
CE11	Carbohydrate esterase family 11	1_1738
GT2	Glycosyltransferase family 2	1_759
GT5	Glycosyltransferase family 5	3_4
GT9	Glycosyltransferase family 9	1_999
GT19	Glycosyltransferase family 19	1_1807
GT28	β -1,4-GlcNAc Transferase	1_1732
GT30	Glycosyltransferase family 30	1_855
GT35	Glycogen and starch phosphorylase	1_1193
GT41	N-glycosyltransferase	1_943
GT51	Murein polymerase	2_71